Informal document WP.5/GE.3 (2019) No. 2

Distr.: General
24 January 2019

English only

Economic Commission for Europe

Inland Transport Committee

Working Party on Transport Trends and Economics

Group of Experts on Climate Change Impacts and Adaptation for Transport Networks and Nodes

Sixteenth session
Geneva, 29 and 30 January 2019
Item 4 of the provisional agenda
Discussions on the final report of the Group of Experts

Climate Change: Trends and Projections

Submitted by Prof. Adonis Velegrakis, University of Aegean

This document provides the draft text for the section1 of chapter 2 of the final report. The Group of Experts will be invited to discuss it and make suggestions and give directions for its further elaboration in the final report.

1. Climate Change: Recent Trends and Projections

The information presented here focuses on climatic factors and hazards the variability and change of which can impact the transportation networks, including temperature and precipitation, snow, glacier and sea ice, and sea level as well as extreme events. Information on their trends and projections until 2013 has been presented in a previous UNECE report (ECE, 2013). In the present (draft) report, focus is placed on the post 2013 trends and most recent projections on Climate Variability and Change (CV & C)[1] which have affected and/or will affect the UNECE region and its transportation.

1.1 Climate Variability and Change Trends

There is overwhelming evidence for a warming world since the 19th century from independent scientific observations in different environments (from the upper atmosphere to the ocean deeps). However, in most cases, discussions on CV & C focus on the land surface temperature increase, which is just one of the indicators of changing climate, with others being changes in e.g. the atmospheric/oceanic temperature, sea level, precipitation, and glacier, snow and sea ice covers (Fig. 1).

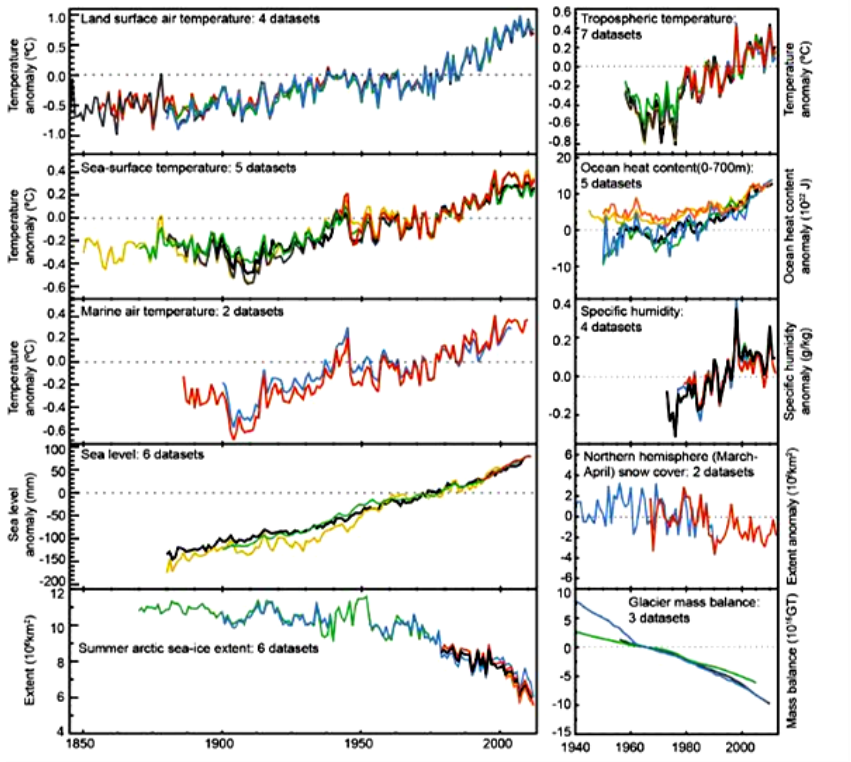

Figure 1 *Change of climatic factors. Each line represents an independently derived estimate. In each panel all data sets have been normalized to a common period of record (IPCC, 2013).*

[1] Note that Climate Variability and Change (CV & C) refers to the variability and sustained change of climatic conditions relative to a reference period, e.g. the first period with accurate records (1850s-1860s) or periods at which infrastructure used today has been constructed (e.g. 1961-1990 or 1986-2005).

Temperature increases have been observed in the troposphere during the last decades. The oceans, which may have absorbed more than 80 % of the excess energy associated with the increased emissions since the 1970s, show also very significant increases in heat content (IPCC, 2013; Melillo et al., 2014; Dieng et al., 2017; Cheng et al., 2019a); these have resulted in steric sea level increases that are considered as a major driver of mean sea level rise-SLR (Hanna et al., 2013). At the same time, glacier and sea ice covers have been declining over the last few decades. Arctic sea ice has shrunk by more than 40 % since satellite records began (1979) at the end (September) of the annual melt season (Melillo et al., 2014; NOAA, 2017a). Glacier ice has also been consistently decreasing during the last 20 years and spring snow cover extent (SCE) has also shrunk across the Northern Hemisphere-NH since the 1950s (IPCC, 2013; NSIDC, 2017).

1.1.1 Temperature and Precipitation

Globally-averaged, near-surface temperature change is the most cited indicator of climate change as it is directly related to both the climate change causes, i.e. the increase in cumulative Greenhouse Gas-GHG emissions (IPCC, 2013) and the planetary energy balance (Fourier 1827), and many impacts and risks (Arnell et al., 2014). Although each year (or decade) has not been always warmer than the previous, there has been a long-term warming trend, with most of the warming having occurred in the past 35-odd years (Fig. 2).

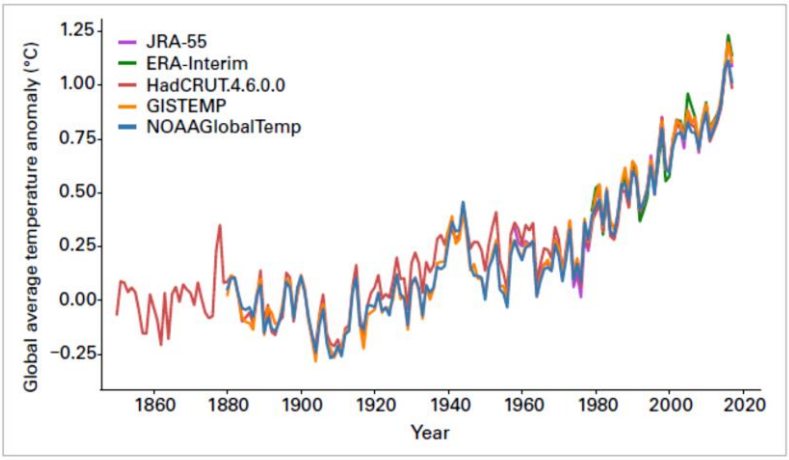

Figure 2 *Global mean temperature anomalies, with respect to the 1850–1900 baseline, for the five global datasets (Source: UK Met Office Hadley Centre). In the individual datasets, 2017 was second warmest in the reanalysis datasets ERA-Interim and JRA-55. (WMO, 2018).*

The five warmest years ever recorded have all occurred since 2010 (WMO, 2018). The five-year mean temperature for 2013–2017 (Fig. 3), which gives a longer-term perspective on the evolving temperatures, has been 0.4 °C above the 1981–2010 average and 1.0 °C above pre-industrial values; it is also the highest on record.

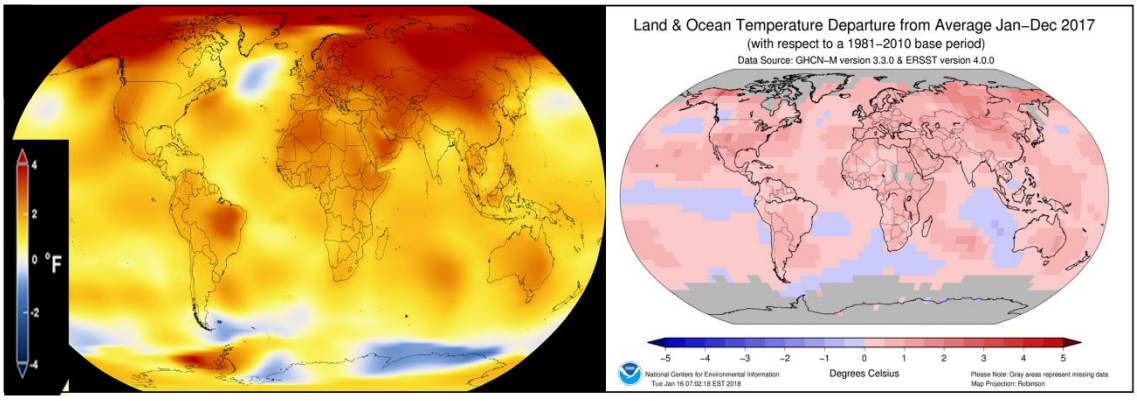

Figure 3 *Average global temperature 2013-2017, as compared to the average of 1951 – 1980 (left) (NASA Goddard Institute for Space Studies, https://climate.nasa.gov/news/2671/long-term-warming-trend-continued-in-2017-nasa-noaa/); and land and ocean departure temperature anomalies in 2017 compared to the 1981-2010 average (right) (NOAA, 2018).*

Warming of the climate system is unequivocal. All observations suggest increases in global average surface air and ocean temperatures which appear to have been largely driven by increased atmospheric concentrations in GHGs (IPCC, 2007; 2013). Global mean temperatures in 2017 were 1.1 °C ± 0.1 °C above pre-industrial levels, having also been considerably warmer than the average of the period 1981 – 2010 (Fig.3). 2017 was the warmest year on record not influenced by an El Niño event (WMO, 2018), whereas 2016 was the warmest year in the instrumental record, breaking the previous record of 2015 (NASA, 2016) and 2014 (MetOffice, 2014). The evidence is consistent with a steady global warming trend since the 1970s, superimposed on random, stationary, short-term variability (Rahmstorf et al., 2017).

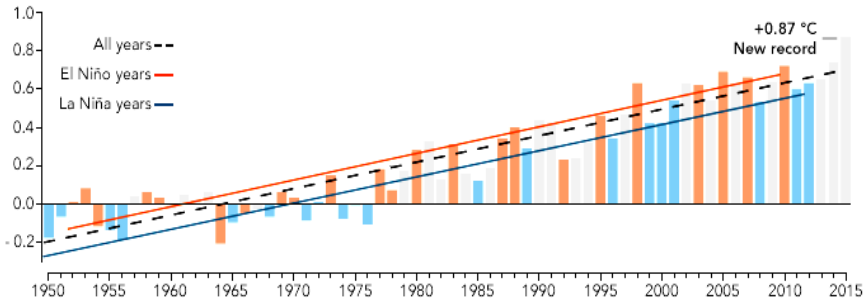

Figure 4 *Annual temperatures compared to 1951-1980 average. Blue and red bars represent the annual temperature anomalies in El Niño and La Niña years, respectively. Blue and red lines are the trends; neutral years in grey; the dashed line represents the overall trend (NASA, 2016).*

Generally, El Niño years are warmer than non El Niño years, i.e. neutral or La Niña years (Fig. 4). The 2015 and 2016 temperature records were influenced by the strong El Niño conditions in the Pacific (NASA, 2016). 2014, which was a neutral El Niño year, showed near surface land temperatures 0.88 ± 0.2 ^{0}C higher than the 1961–1990 average (WMO, 2014).

Over the period 2003–2013 there was an apparent slowdown in the rate of the global mean (surface) temperature rise compared to global climate model projections (Dieng et al., 2017a). This slowdown (‘*the*

global warming hiatus') was attributed to uncertainties in the simulations of the conventional datasets and processes related to 'external' climate forcing, such as volcanic eruptions, stratospheric changes in water vapor and industrial aerosols, heat redistribution within the oceans, solar activity and the inter-annual to decadal variability of ocean cycles (IPCC, 2013; MetOffice, 2014; Fyfe et al., 2016; Yan et al., 2016; Cheng et al., 2019). Recent research (e.g. Cowtan and Way, 2014; Karl et al, 2015; Simmons et al., 2017) has even questioned the presence of a *hiatus* in the temperature trend; re-analysis of the updated and corrected for biases datasets has indicated higher global temperature trends in the *hiatus* period than those previously reported (e.g. IPCC, 2013).

Climate is controlled by the heat inflows and outflows and its storage dynamics in the various constituents of the Earth System, i.e. the ocean, land and atmosphere (IPCC, 2013). Most of the heat storage occurs in the ocean, as it absorbs most of the heat added to the climate system (Cheng et al., 2019a) and, thus, changes in ocean temperature are important indicators of climatic changes. In recent years, there has been ample evidence of an increasing ocean heat content, with the rate being estimated as 0.64 Wm^{-2} for the period 1993-2008 (Lyman et al., 2010) and 0.5 – 0.65 Wm^{-2} for the period 2003-2013 (Dieng et al., 2017a). Temperature rises have been observed down to depths of 3000 m since 1961 (IPCC, 2013). In any case, the past 5 years (2014-1018) have been the 5 warmest on record for the upper ocean (Cheng et al., 2019b). There is also a correlation between the increase in ocean heat content and the sea level rise (Fig. 5) due to the steric effects-thermal expansion (NASA, 2016).

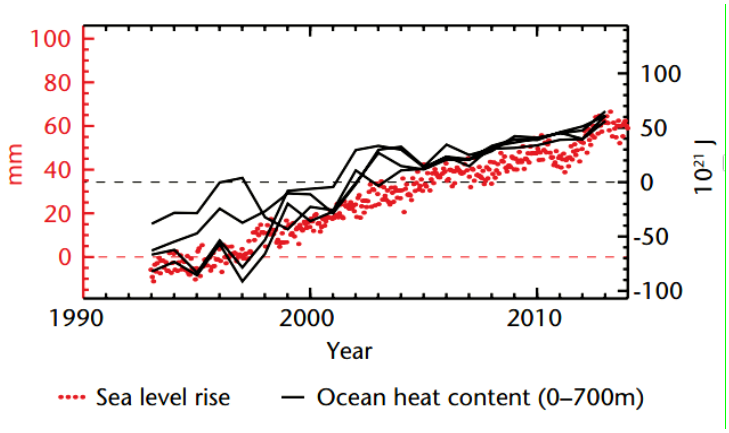

Figure 5 *Global average sea level rise and change in ocean heat content for 1993-2013. Sea-level data from TOPEX (1993–2001), Jason-1 (2002–08) and Jason-2 (2008–13) (http://sealevel.colorado.edu/). Ocean heat content (upper 700 m) relative to the 1993–2012 average. Data from CSIRO/ACE CRC, PMEL/JPL/JIMAR, NODC, and EN4.0.2 (MetOffice, 2014).*

Analysis of global land precipitation data reveal that there was an increasing trend since the 20th Century, especially in middle and high latitudes (low confidence before 1951, medium confidence afterwards) (EPA, 2015). When only the mid-latitudes in the Northern Hemisphere (NH) are considered, confidence in the precipitation trends for the years after 1951 becomes high. Global precipitation shows mixed long term trends and strong regional variability. Heavy precipitation events (downpours) have increased in intensity and/or frequency in many parts of Europe and N. America, whereas there has been also an increased frequency and intensity of droughts in the Mediterranean and parts of Africa (IPCC,

2013). Schneider et al. (2017) applied mean weather-dependent corrections to precipitation data from 75,100 meteorological stations (Global Precipitation Climatology Center-GPCC) and found a mean annual precipitation of about 855 mm (excluding Antarctica) for the period 1951-2000; they also suggested that a warming of about 1 ^{0}C relative to pre-industrial time could result to a 2 - 3 % increase in global precipitation.

In the periods 1931–1960 and 1941–1970, there were larger differences compared to those in the 1951–2000 period; more rainfall occurred over West Africa and less over the SE Asia and Indonesia (Meyer-Christoffer et al., 2015). In Europe and N. America, precipitation decreased in the south and increased in the north. In Spain, for example, precipitation patterns have changed in recent decades: dry periods became lengthier, annual rainfall decreased by up to 15 %, and the number of heavy precipitation events decreased (Valdez- Abellan et al., 2017). Precipitation decreased in the most recent 30-year period in August, September and October, which might be related to the more frequent (El Niño Southern Oscillation - ENSO) events and weakened Indian and Southeast Asian summer monsoons (Schneider et al., 2017).

1.1.2 Snow and Sea Ice

The snow cover extent (SCE) in the North Hemisphere (NH), i.e. about the 98 % of the global snow cover, has declined by 11.7 % per decade in June (EEA, 2015a) over the period 1967-2012. However, the trend is not uniform. Some regions (e.g. the Alps and Scandinavia) showed consistent decreases in the snow cover depth at low elevations but increases at high elevations, whereas in other regions (e.g. the Carpathians, Pyrenees, and Caucasus) there were no consistent trends (EEA, 2012). In the Arctic region, there has been a downward trend in the extent and duration of snow cover over the past few decades.

1 Arctic sea ice is also in decline (Figs 1 and 6). Sea ice usually expands during the cold season to a March-April maximum, and then contracts during the warm season to a September minimum. By comparison, Antarctic sea ice shows its minimum extent in February-March and expands during the South Hemisphere cold season to a September maximum. Minimum Arctic sea ice extent has declined by about 40 % since 1979 with the most records in ice minima having occurred in the last decade (NOAA, 2017a).

The (land) ice mass balance of Antarctica (and Greenland) is extremely important as it controls (amongst others) the mean sea level ice (SLR). All information indicates that the Greenland Surface mass balance-SMB showed no significant trend from the 1960s to the 1980s, but started to show a decrease since the early 1990s (on average by 3 % per year). This has resulted in a statistically significant and increasing contribution to the rate of mean SLR (Hansen et al., 2016). The long-term trend for the Antarctic ice appears flat (Fig. 7). Recently, however, there have been worrying signs. It appears that the total mass loss increased from 40 ± 9 Gt year^{-1} in 1979 - 1990 to 50 ± 14 Gt year^{-1} in 1989 – 2000, to 166 ± 18 Gt year^{-1} in 1999 – 2009, and to 252 ± 26 Gt year^{-1} in 2009 – 2017. The contribution to sea-level rise from the land ice mass melt of Antarctica averaged 3.6 ± 0.5 mm per decade with a cumulative 14.0 ± 2.0 mm since 1979 (Rignot et al., 2019).

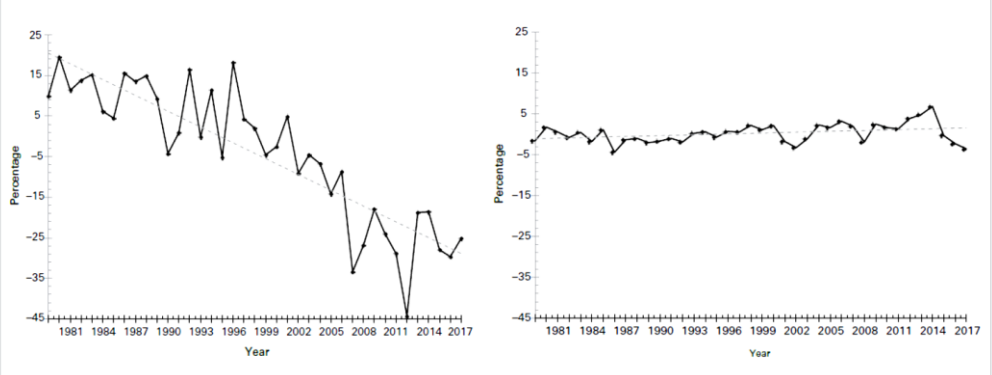

Figure 6 *September sea ice extent (SIE) for the Arctic (minimum, left) and Antarctic (maximum, right): Percentage of long-term average of the reference period 1981–2010 (US National Snow and Ice Data Center data) (WMO, 2018).*

1.1.3 Sea Level

During the last decades, a significant rise of the mean sea level has been observed due to: (a) ocean thermal expansion (OTE), i.e. ocean volume changes due to steric effects; (b) glacio-eustasy i.e. ocean mass increases from the melting of the Greenland and Antarctic ice sheets (GIS and AIS) and the glaciers and ice caps (GIC); (c) glacio-isostatic adjustment (GIA); and (d) changes in terrestrial water storage (e.g. Hanna et al., 2013). The rate of global SLR increased sharply above the relatively stable background rates of the previous 2000 years (Church and White, 2006; Engelhart et al., 2009; Gehrels and Woodworth, 2012; Horton et al., 2014).

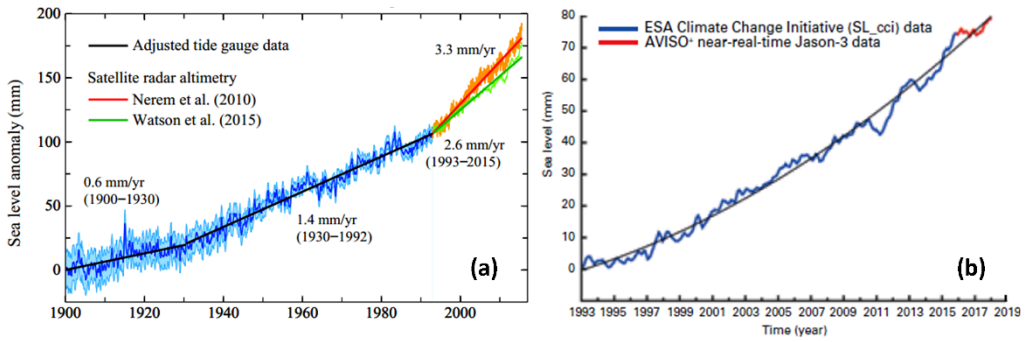

Figure 7 *(a) Estimated sea level change (mm) since 1900. Data through 1992 are the tide-gauge record of Church and White (2011) with the change rate multiplied by 0.78, so as to yield a mean 1901–1990 change rate of 1.2 mm year^{-1} (Hansen et al., 2016). (b) Global mean sea-level (with seasonal cycle removed), January 1993–January 2018, from satellite altimetry multi-missions. Data from AVISO (Source: Collecte-Localisation-Satellite (CLS) – Laboratoire d'Etudes en Géophysique et Océanographie Spatiales (LEGOS) (WMO, 2018).*

Since 1860, global sea level has increased by about 0.20 m; during this period, global SLR rates averaged 1.3 to 1.8 cm per decade (Church et al., 2013; Hay et al., 2015). However, SLR rates have become progressively greater; there is a discernible acceleration in the global SLR since the 1900s that has intensified in the past 25 years (Fig. 7).

As with temperature, the upward trend in sea level has varied over the decades. For example, there were lower rates of increase during the early part of the 20th century and most of the 1960s and 1970s; sea level increased more rapidly during the 1930s and through the 1950s. Recently, satellite and tide gauge observations indicate a global SLR of 3.3 ± 0.25 cm per decade since 1993 (Church et al., 2013). It has been suggested that the increase is mainly due to ice mass balance changes (Section 1.1.2) rather than steric effects (Dieng et al., 2017b; Rignot et al., 2019).

There is considerable regional (spatial) variability in the coastal SLR (Menendez and Woodworth, 2010). In Europe, sea levels have increased along most of its coast in the last 40 odd years, with the exception of the N. Baltic coast (EEA, 2012). Some regions experience greater SLR than others. In the tropical western Pacific high SLRs were observed since 1993 that may have contributed in the devastation of Philippines by the *Haiyan* typhoon storm surge (November 2013). SLR and variations in regional climate have also led to changes in the distribution/ trends of extreme sea levels (ESLs) since the late 20th century (WMO, 2016).

1.1.4 Extreme Climate Events

Climate change is often characterized in the public discourse by the increase in global mean temperature. However, for the transportation industry and the society, economy and the environment, regional conditions and changes in the extremes, such as heat waves, droughts, or floods, can be most relevant (Vogel et al., 2017). Changes in the mean climate can lead to changes in the frequency, intensity, spatial coverage, duration, and timing of weather and climate extremes, potentially resulting in unprecedented extremes. These extremes can, in turn, modify the distributions of the future mean climatic conditions (IPCC SREX, 2012).

Extreme events (e.g. storms, floods, droughts and heat waves) as well as changes in the patterns of particular climatic systems (e.g. the monsoons) (King et al., 2015) can be, at smaller spatio-temporal scales, the most impacting climatic phenomena, since they may induce abrupt and more severe effects/natural disasters than changes in the mean climatic factors. Moreover, societies are rarely prepared to efficiently face extreme weather events, having become dependent on predictable, long-term climatic patterns (MetOffice, 2014). Extreme hydro-meteorological events cause on average about 650 deaths annually in the USA and are responsible for some 90 % of all President-declared disasters. A substantial slice of the economy (value of about US$3 trillion) appears to be sensitive to weather and climate; since 1980, the USA has sustained more than 200 hydro-meteorological disasters with a total cost exceeding $1.1 trillion (NOAA, 2017c).

Many indicators of climate extremes show changes consistent with global warming, including a widespread reduction in the number of frost days in mid-latitude regions and discernible evidence that warm extremes have become warmer and cold extremes less cold in many regions (IPCC SREX, 2012). Evidence suggests a general change in the frequency of high impact temperature and precipitation extremes over land, irrespective of the type of dataset and processing method used (MetOffice, 2014). A slight decrease in the annual number (globally) of mild days (i.e. days with maximum temperature between 18 - 30 °C and precipitation < 1 mm) is projected for the near future (4 days/year for the 2016 - 2035 and 10 days/year for the 2081 - 2100) (Van der Wiel et al., 2017).

Extreme events have consequences which are difficult to predict. Their variability covers a large spectrum, such as sudden and transient temperature changes, rapid retreats of sea ice, bouts of

abnormally high precipitation, intensive storms, storm surges, extended droughts, heat waves and wildfires and sudden water releases from melting glaciers and permafrost slumping that may have substantial and costly impacts on transport infrastructure and operations. There is evidence indicating that extreme events, such as tropical and temperate storms, may respond to a warming climate by becoming more extreme (e.g. Emanuel, 2005; Ruggiero et al., 2010; WMO, 2014). For example, a modest increase by 1 °C in the ocean temperature may result in increases of the wind speed of tropical cyclones by 5 m/s which may result in increases in the incidence of the most intense and destructive (Category 5) cyclones (e.g. Steffen, 2009). It appears that although the number of hurricanes has not been significantly changed with time (Fig. 8), their ferocity (and impacts) have increased due to the increase in the ocean's heat content and temperature (Trenberth et al., 2018). The implications of these extreme events for e.g. the coastal communities and transport infrastructure could be severe, as they may increase (amongst others) the likelihood of higher extreme sea levels (ESLs) from storm surges/waves (Stockdon et al., 2012; Vousdoukas et al., 2018; Monioudi et al., 2018) and coastal floods.

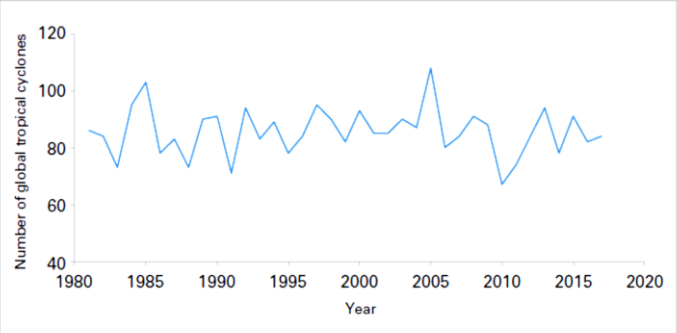

Figure 8 *Total number of tropical cyclones globally, by year (WMO, 2018)*

In addition, changes in the intensity and frequency, and/or changes in the patterns, of extreme waves (e.g. Ruggiero, 2013; Bertin et al., 2013; Mentaschi et al., 2017) may also induce, at least temporarily, coastal erosion or inundation, particularly when combined with increasing mean sea levels (e.g. Losada et al., 2013; Vousdoukas et al., 2017). Storm surges pose a particular threat to highly developed coastal areas, particularly low-lying estuarine coasts such as the Rhine, Danube and the Mississippi river deltas that are considered hotspots of coastal erosion/vulnerability due to their commonly high relative SLRs (ECE, 2013).

In Southern Europe, analysis of (tide gauge) observations has shown that changes in extreme water levels tend to be dominated by the mean sea level rise (SLR) (Marcos et al., 2011). Coastal areas currently experiencing erosion and/or inundation are projected with high confidence that will continue to do so in the future, due to increasing sea levels, all other contributing factors being equal (Hallegatte et al. 2013; Vousdoukas et al., 2017). The projected increases in ESLs constitute a serious threat to global coastal societies, the safety and resilience of which depend on the effectiveness of the natural and man-made coastal flood protection structures present (e.g. Velegrakis et al., 2016; Ranasighe, 2016).

One of the clear trends appears to be the increasing frequency and intensity of heavy precipitation events (downpours). The increase has caused most of the observed increases in overall precipitation during the last 50 years and projections from climate models suggest that these trends will continue in this

century. Slope failures/landslides have also increased at mountainous areas, as they are linked to heavy downpours (Karl et al., 2009).

River flooding is a most serious and widespread hazard (King et al., 2015). Between 1980 and 2014 river floods accounted for 41 % of all loss events, 27 % of fatalities and 32 % of economic losses (Munich Re, 2015). Recently, the flooding caused by the extremely heavy downpours during the Hurricanes *Harvey* (2017) and *Florence* (2018) was particularly destructive for the southern and eastern USA (Section 1.1.5). Riverine floods are caused by both physical and socio- economic factors. The former depend on the hydrological cycle, which is influenced by changes in temperature, precipitation and glacier/snow melts, whereas the latter by land use changes, river management schemes, and flood plain construction (EEA, 2010). In the ECE region, floods are an ever present threat (Fig. 9).

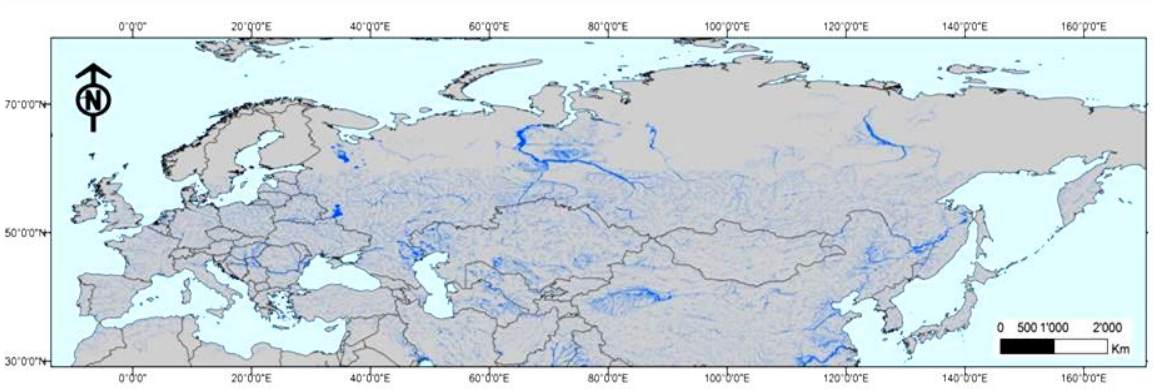

Figure 9 *Current flood hazard (95 % probability) in the Eurasian region of the ECE for the 100-year flood from a global GIS model based on river discharge time-series. DEM resolution 90 m. Areas over 60 ^{0}N are not fully covered (From UNEP-GRID and UNISDR, 2008). (ECE, 2013)*

The current trends in the Eurasian countries show a significant flood hazard (for the 1 in a 100-year event), particularly for central and eastern Europe, the central Asia and along the large S-N trending Siberian drainage basins (Fig. 9). Changes in extreme hydrological events and their impacts are better studied at a regional/local scale, with most existing studies focusing on the generation and impacts of floods due to e.g. increases in torrential precipitation.

In Europe, annual water discharges have generally increased in the north and decreased in the south (e.g. EEA, 2012), trends that are projected to hold in the future (Alfieri et al., 2018) as they are related to the projected precipitation changes (EEA, 2015c). By 2050, there is at least a 50 % chance that climate change alone would lead to a 50 % increase in flooded people across sub-Saharan Africa, and a 30 to 70 % chance for such an increase in Asia. By 2100 the risks have been projected to be much greater (King et al., 2015).

There is also evidence to suggest increases in the frequency and intensity of heat waves (e.g. Beniston and Diaz, 2004; IPCC, 2013); generally, there has been a 3-fold increase since 1920s in the ratio of the observed monthly heat extremes to that expected in a non-changing climate (Coumou and Rahmstorf, 2012). With mean temperatures continuing to rise, models project that increases in the frequency/magnitude of hot days and nights and decreases in the cold days and nights are virtually certain (IPCC, 2013). For example, most of North America appears to have experienced more unusually hot days

and nights, fewer unusually cold days and nights and fewer frost days (ECE, 2013). Heat waves are often associated with severe droughts (as in the European 2003 heat wave). Droughts have become more severe in some regions, a trend that projected to hold (and, possibly, increase) in the 21st century (IPCC, 2013).

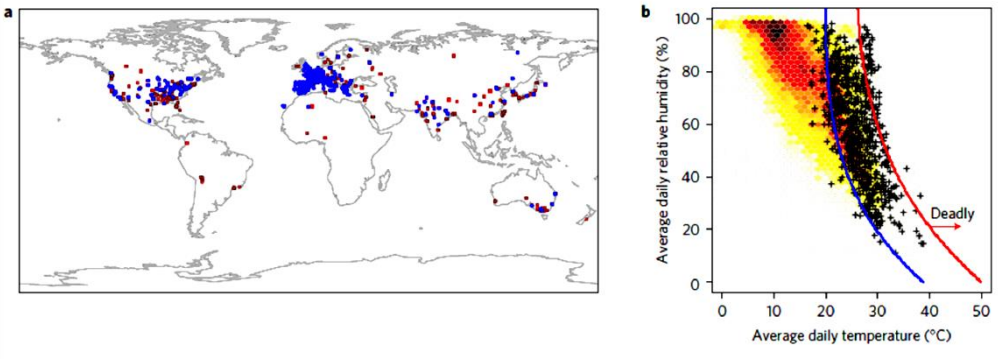

Figure 10 *Lethal heat events (1980-2014). a, locations with documented relationships between heat and mortality (red squares) and where specific heat events have been studied (blue squares). b, mean daily surface air temperature and relative humidity during lethal events (black crosses) and during periods of equal duration from the same locations but from randomly selected dates (I,e, non-lethal events; red to yellow). Blue line is the threshold that best separates lethal and non-lethal events; red line is the 95% probability deadly threshold (Mora et al., 2017).*

It should be mentioned that in many cases the hazard related to the extremes of a particular climatic factor can be exacerbated by the simultaneous presence of another hazard(s), such as combined marine and riverine flooding (Forzieri et al., 2016). A combined hazard which might have very significant implications for the health/safety of personnel and passengers in most modes of transport is the combination of extreme heat with high relative humidity -the Heat Index (e.g. Monioudi et al., 2018). Recent research (Mora et al., 2017) indicates the presence of a 'deadly threshold' for the surface air temperature/relative humidity over which the human thermoregulatory capacity is exceeded (Fig. 10). Around 30 % of the world's population is currently exposed to climatic conditions exceeding this deadly threshold for at least 20 days a year and projections suggest that there will be a very significant deterioration in the course of the century (see also Section 1.2.4).

1.1.5 Climatic factors during the most recent period

Temperature and Precipitation

As mentioned earlier the most recent five year period for which there is complete information (2013–2017) has been the warmest on record (0.4 °C above the 1981–2010 average and 1.0 °C above pre-industrial values). Global temperatures were consistent with a warming trend of 0.1 - 0.2 ^{0}C per decade, with most Eurasia being warmer than average (WMO, 2017).

In 2017 global land temperature was 1.31 °C above the 20th century average and also the third highest in the 138-year record, behind only 2016 and 2015. Sea temperatures also soared, averaging 0.67 °C above the 20th century average (WMO, 2018). It is noteworthy that the integrated global land and ocean temperature in March 2017 was 1.03 °C above the 20th century average; this was the first time the monthly

temperature anomaly surpassed 1.0 °C in the absence of an El Niño event. The average global temperature integrated across both land and ocean surface areas was 0.84 °C above the 20th century average of 13.9 °C [2].

2016 was the warmest year on record for both land and oceans and for both hemispheres, due to the El Niño event that started in 2015 and continued into 2016 (NOAA, 2017b). Global average temperature was 0.83 ± 0.10 °C higher than the average of the 1961 – 1990 and about 1.1 °C above the pre-industrial time. Record temperatures were widespread at the NH, particularly in Arctic regions (Fig. 11). In early 2016, global temperature was about 1.5 °C above that recorded in the early industrial revolution and > 0.4 °C higher than that recorded in 1998 (a strong El Niño year) (Simmons et al., 2017)[3]. Alaska experienced unprecedented, widespread warming (NSIDC, 2017). Globally averaged sea surface temperatures (SSTs) were also the warmest on record, with the anomalies being highest in early 2016 (WMO, 2017). Overall, the 6 highest monthly temperature anomalies in the record have all occurred in the period September 2015 - February 2016 (NOAA, 2016d). A vast NH region stretching from central Russia into eastern Europe as well as Alaska showed temperatures in February more than 5 °C above the 1981 – 2010 average.

2015 was the first year that global average temperatures were recorded as 1 °C or more above the 1880-1899 average (NOAA, 2017b). Sea surface temperatures (SSTs) were also above average in most of the oceans, with the exception of some areas in the Southern Ocean and the eastern South Pacific. In the most recent period, warm temperatures also occurred in the subsurface waters, with the integrated ocean heat content within the 0 - 700 m ocean layer being higher since 2013 - 2014 than previous times (NOAA, 2016). There were two notable ocean temperature anomalies in late 2013: (i) a large area of very warm water (> 2 °C above average) in eastern North Pacific; and (ii) a persistent pool of water exhibiting SSTs below-normal in eastern North Atlantic.

Land precipitation was strongly influenced by the El Niño-Southern Oscillation (ENSO). The recent 5-year period followed a strong La Niña year (2011 - early 2012) that produced very wet conditions; 2011 was assessed by NOAA as the second-wettest year on record. However, 2013 and 2014 were close to the long-term average. The western US, eastern Australia and Brazil had large areas where rainfall in October 2012 - September 2015 was below the 10th percentile, whereas there were also regions where precipitation exceeded the 90th percentile (e.g. in eastern Russia). In Europe, there was a marked north/south split, with wet conditions in Scandinavia and dry conditions in much of the central and SE Europe. Major annual precipitation anomalies were less common in 2013 and 2014, with significant anomalies observed in SE Europe (2014). In 2014, very dry conditions occurred over much of the central US and central and western Russia.

[2] See also https://www.ncdc.noaa.gov/sotc/global/201713

[3] An alarming development in view of the 2015 Paris Agreement the aim of which is to 'hold' the global average temperature increase to well below 2 ^{0}C above pre-industrial levels (UNFCCC, 2015, IPCC, 2018).

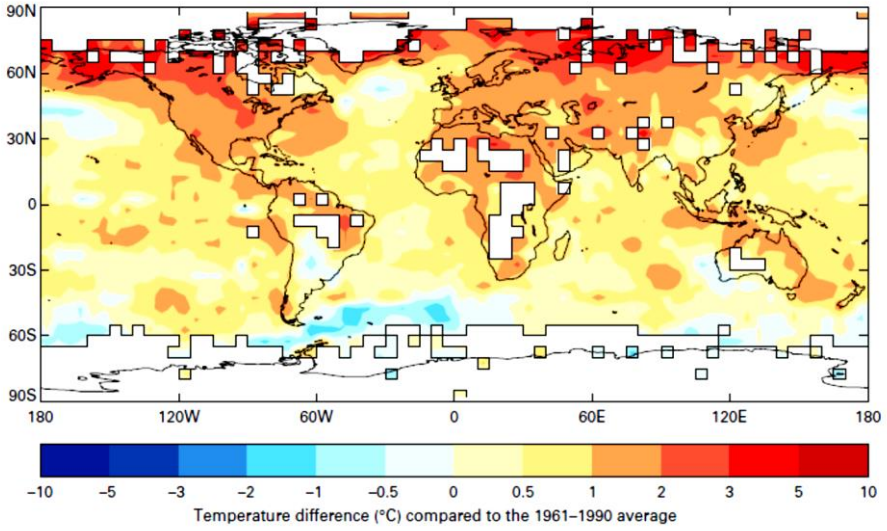

Figure 11 G*lobal temperature anomalies in 2016 (relative to the 1961–1990) (WMO, 2017).*

In 2016, global precipitation was influenced by the transition from the El Niño conditions in the early year to the neutral or weak La Niña conditions in the second half of the year. This resulted in strong seasonal contrasts (but annual totals close to the average conditions) in many regions. In other regions, however, heavy post-El Niño rainfall resulted in annual precipitation above average; 2016 was a wet year in many high-latitude NH areas (WMO, 2017). Precipitation above the 90th percentile was observed in a large swath of the UNECE region extending from Kazakhstan across the western Russian Federation into Finland, northern Sweden and Norway. However, large areas of the northern-central Russian Federation were dry, with much of the region between the Urals and Lake Baikal and to the north of 55 ^{0}N having precipitation below the 10th percentile. Another non-typical region was California, where the 2015 - 2016 seasonal rainfall was near average (after 4 very dry years), increasing towards the end of the year. Precipitation was also close to average over most of central and western Europe, but with a very wet first half and a dry second half of the year. Belgium is a particular example of the high variability in the 2016 precipitation: some areas had their wettest January–June period on record (62 % above average), followed by the third-driest July–December period on record (36% below average) (WMO, 2017). In 2017, there were fewer areas with large precipitation anomalies than there had been in the previous years, as the influence of the strong El Niño of 2015 - 2016 ended (WMO, 2018).

Snow and Ice

The cryosphere component of the Earth system includes solid precipitation, snow cover, sea ice, lake and river ice, glaciers, ice caps, ice sheets, permafrost and seasonally frozen ground. The cryosphere provides most useful indicators of climate change, yet is one of the most under-sampled domains of the Earth system. There are at least 30 cryospheric properties that should be (ideally) measured. The major cryosphere elements for which assessment is here provided include the snow cover, sea ice, glaciers and ice sheets and the permafrost state. The assessment of the current state, trends and future evolution of the cryosphere is particularly important for transportation in the UNECE region, as large areas in the Arctic (e.g.

in the Russian Federation, Canada and the USA) with large natural resources as well as the Arctic Ocean are affected.

Despite the overall high temperatures of the most recent period, there were still episodes of abnormal cold and snow in the NH. A prolonged period of extreme cold affected Europe in early 2012, the worst cold spell since 1987 in central and western Europe. March 2013 was also notably cold in much of Europe, with significant blizzards in some locations. The winters of 2013 - 2014 and 2014 - 2015 were significantly colder than normal in many areas of the central and eastern US and southern Canada, with persistent low temperatures for extended periods. In February 2015, temperatures in Montreal, Toronto and Syracuse did not rise above 0 ^{0}C. In coastal regions there were frequent snowfalls, resulting in Boston experiencing its highest seasonal snowfall on record (WMO, 2016).

Mean annual snow cover extent (SCE) for 2016 in the NH was 24.6 million km^2, 0.5 million km^2 below the 1967–2015 average, despite the winter snow storms that moved across N. America in January; this was very similar to 2015 (e.g. NOAA, 2017a). In Eurasia, the winter SCE was 270,000 km^2 below average. In April, the mean SCE was the lowest on record, although autumn SCE was above average (WMO, 2017). In 2017, the SCE in NH was close or above the 1981–2010 average for most of the year, most significantly in May (9 % above average, the highest since 1985) particularly in northwestern Russia and Scandinavia. However, the summer SCE was close to the long-term average (WMO, 2018).

Arctic sea-ice extent (SIE) was at record low levels for much of 2016. The seasonal maximum of 14.52 million km^2 (24th March) was the lowest in the 1979 – 2016 satellite record, below that of 2015; notable exceptions were observed in the Labrador Sea, Baffin Bay and Hudson Bay. Arctic SIE dropped to record lows in May - June, but a slow summer melt resulted in a seasonal minimum of 4.14 million km^2, above the 2012 record. When averaged for the year, Arctic SIE was 12.6 % below average, with maximum and minimum SIE being 1.12 and 2.08 million km^2 below the 1981-2010 average, respectively. Large areas of the open ocean in e.g. Beaufort, Chukch, Laptev and East Siberian Seas had a minimum ice extent in mid-September (WMO, 2017). Antarctic SIE was close to the 1979 – 2015 average for the first 8 months of 2016, reaching a seasonal maximum of 18.44 million km^2 in late August (the earliest seasonal maximum on record). However, following an exceptionally rabid spring melt the November SIE was 14.54 million km^2, by far the lowest on record (1 million km^2 below the previous record) (WMO, 2017). The reasons behind the SIE collapse in late 2016 are not yet understood, having been described as a "*black swan*" event (NSIDC, 2017).

In 2017, SIE was also well below the 1981 – 2010 average in both the Arctic and Antarctic. The winter maximum of Arctic SIE of 14.42 million km^2 (7th March), was the lowest winter maximum in the satellite record, below the previous record of 2015. However, the spring/summer melt was slower than in recent years. The summer end minimum of 4.64 million km^2 (13th September) was about 1.25 million km^2 over the 2012 record low (WMO, 2018).

Greenland's ice sheet mass was assessed by Velicogna et al. (2014) who found a loss rate of 280 ± 58 Gt year^{-1}, accelerating by 25.4 ± 1.2 Gt year^{-1}. Ice mass loss of 74 ± 7 Gt year^{-1} was also observed in the nearby

Canadian glaciers and ice caps with an acceleration of 10 ± 2 Gt year^{-1} [4]. Mountain glaciers generally continued their melt. The vast majority (25 out of 26) reference glaciers for which 2015 - 2016 data are available shows ice mass deficits, which are less extreme than those of 2014 - 2015, but above the 2003 – 2015 average (WMO, 2017). In recent years, the Western North American (WNA) glaciers have lost 117 ± 42 gigatons (Gt) of mass, showing a fourfold increase in loss rate between 2000 – 2009 (2.9 ± 3.1 Gt yr^{-1}) and 2009 -2018 (12.3 ± 4.6 Gt yr^{-1}); this may be due to a shift in regional meteorological conditions driven by the location and strength of upper level zonal wind (Menounos et al., 2018). Recent research has suggested also a rapid acceleration in 2009 – 2017 in the Antarctic ice mass loss (to 252 ± 26 Gt year^{-1}) (Rignot et al, 2019). There was also warming down to 20 m depth in Arctic permafrost regions. Temperatures have increased in most regions by up to 2 ^{0}C since 1980, leading to thawing and significant infrastructure damage; the thickness of the NH permafrost has decreased by 0.32 m since 1930 (IPCC, 2013).

Sea Level Rise

In recent years, mean sea level continued to rise. In early 2012 global sea level was about 10 mm below the long-term trend (probably due to the strong La Niña); however, by mid-2012, the mean sea level trend had rebounded. A marked rise occurred in early 2015 (as the 2015 - 2016 El Niño developed), with sea levels being about 10 mm above the long-term trend (see Fig. 7).

SLR over the full satellite record (1993-2017, about 3.3 mm year^{-1}) has been considerably higher than the average of the 1900 - 2010. There is evidence suggesting that the contribution to SLR from the continental ice sheet melt, particularly from those of Greenland (GIS) and west Antarctica (WAIS), has been increasing (Velicogna et al., 2014; Rignot et al., 2019). For example the contribution of GIS melting to global SLR in the 2011 - 2013 period (that includes the extreme melt year of 2012) was approximately 1 mm year^{-1}, well in excess of the 0.6 mm year^{-1}estimated for the period 2002 - 2011 (IPCC, 2013). In the Pacific Ocean, strong regional differences were apparent since 1993; these have been mostly attributed to ENSO effects. Sea level rise has been more consistent in the Atlantic and Indian Oceans with most areas in both oceans showing rates similar to the global average.

Extreme events

There have been many extreme events such as tropical cyclones, heat and cold waves, floods, droughts and intense windstorms that have affected the UNECE region and its transport infrastructure and operations. Some of these events caused severe damages/losses: the Hurricane *Sandy* in the Caribbean and the US (2012), droughts in the southern and central US (2012 and 2013), floods in central Europe (May-June 2013, Fig. 12) and the 2017 hurricane season. Fortunately, human loss did not follow the upward trend in

[4] These processes have had significant effects on global SLR. Observations indicate that the contribution of Greenland's ice loss has increased from 0.09 (–0.02 - 0.20) mm yr^{-1} in 1992–2001 to 0.59 (0.43 - 0.76) mm yr^{-1} in 2002–2011, while the contribution of Antarctica's ice sheet melt increased from 0.08 (–0.10 to 0.27) mm yr^{-1} in 1992–2001 to 0.40 (0.20 to 0.61) mm yr^{-1} in 2002–2011. Altogether, ice sheet melt contribution to SLR is estimated as 0.60 (0.42 - 0.78) mm yr^{-1} for the period 1993-2010 (IPCC, 2013).

economic losses (Fig. 13). In terms of casualties, Typhoon Haiyan (Yolanda) in the Philippines and flash floods in N. India resulted in 13,600 deaths (2013). More than 3,700 people lost their lives from heat waves in India and Pakistan (May - June 2015)[5]. In terms of economic losses, the 1980 – 2016 average has been 5.5 disaster events per year with costs in excess of 1 US$ billion (CPI-adjusted), whereas the annual average for 2012 – 2016 has been 10.6 such events (NOAA, 2017c).

Figure 12 *Flood damages on European roads in June 2013: (a) Highway 8 in Grabenstaett, S. Germany ((Matthias Schrader, AP); (b) Tyrol, Austria (Kerstin Joensson, AP).*

In 2017, there were very severe extreme events, including a very active North Atlantic hurricane season, major monsoon floods in the Indian subcontinent, and severe droughts in east Africa. These events made 2017 the year with the highest documented economic losses associated with extreme hydro-meteorological events (WMO, 2018). Although the overall number of tropical cyclones (84) was close to the long- term average (Fig. 8), some of them (mainly in North Atlantic) were particularly ferocious.

Three exceptionally destructive hurricanes (Fig. 14) occurred in the North Atlantic in late August - September devastating coastal areas in the southern USA as well as several Caribbean islands including overseas territories of UNECE Member States (e.g. Puerto Rico, the British Virgin Islands, and the Saint Martin and Sint Maarten).

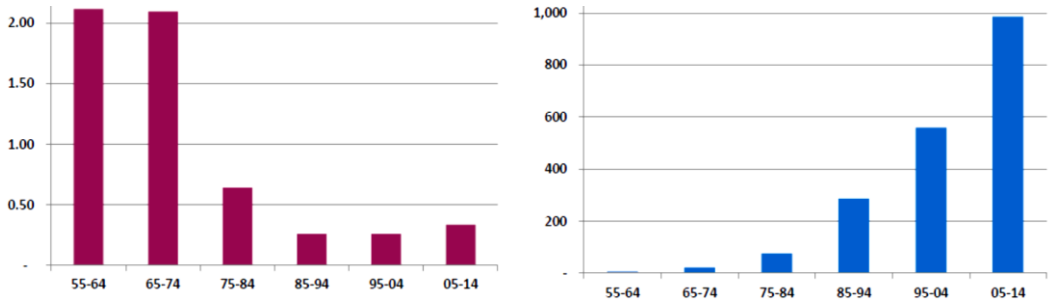

Fig. 13 *Human (left) and economic losses by decade. Economic losses in US$ billions, adjusted to 2013 (NOAA, 2017c).*

[5] The most lethal climatic extreme in recent years has been the 2010-2011 drought in Somalia that caused the 2010 - 2012 Somalia famine, considered responsible for more than 258,000 deaths (WMO, 2016).

Harvey made landfall in south Texas as a category 4 hurricane and remained almost stationary over Houston for several days, producing prolonged downpours and severe flooding (Fig. 14); 1539 mm of rain fell between 25/08/2017 and 01/09/2017 (annual exceedance probability less than 1 in 1000). Trenberth et al. (2018) suggested that this event had been made 3 times more likely by anthropogenic climate change.

Hurricanes *Irma* (category 5, early September) and *Maria* (category 5, mid September) followed. *Irma*'s landfall led to extreme damages across many Caribbean islands (Barbuda, Saint Martin/Sint Maarten, Anguilla, St Kitts and Nevis, the Turks and Caicos, Virgin Islands and the southern Bahamas). *Maria* made initial landfall on Dominica (total damages/losses estimated as US$ 1.3 billion – 224 % of GDP), before it continued towards Puerto Rico where it induced severe and widespread human losses and damages (Fig. 14). The 2017 hurricanes were responsible for more than 320 deaths and were assessed by the National Center for Environmental Information (NCEI) as ranking in the top five for hurricane-related economic losses in the USA (together with *Katrina (*2005) and *Sandy* (2012)*)*, with estimated losses of US$ 125 billion (*Harvey*), US$ 90 billion (*Maria*) and US$ 50 billion (*Irma*) (WMO, 2018).

In 2018, there were also major tropical storms, some of which developed very rapidly. These included Hurricanes *Florence* and *Michael* in the Atlantic and the strong typhoons Jebi, Maria, Manghut (the most intense 2018 storm with winds of 287 km h^{-1}) and Trami in the Pacific. Some of these storms caused major flooding, especially *Florence* (Carolinas, SE USA) and *Olivia and Lane* (Hawaii); *Lane* induced the second-highest rainfall (after *Harvey*) from a tropical cyclone in the USA since 1950 (Cheng et al., 2019b).

Heat waves have been recorded in Europe in 2012, 2013 and 2014. In Austria, it was the first time that temperatures reached 40 °C or above. A prolonged heat wave affected many parts of eastern Asia in July - August 2013 (WMO, 2014). Intense heat waves (temperatures at, or above 45 °C) were recorded in May - June 2015 in India and Pakistan (WMO, 2016). In western and central Europe, the worst heat wave since 2003 was recorded in early July 2015, with Spain, France and Switzerland breaking all time temperature records; a few weeks later, temperatures of 40.3 °C were also recorded in Germany. In 2017 there were also numerous heat waves which affected Turkey and Cyprus in late June - early July, the western Mediterranean (Spain and Morocco) in mid-July, and Italy and the Balkans in early August. All-time records were set in: Antalya, Turkey (45.4 °C on 1st July), Cordoba (46.9 °C on 13th July) and Granada (45.7 °C on 12th July) in Spain; and Pescara (41.0 °C on 4th August), Campobasso (38.4 °C on 5th August) and Trieste (38.0 °C on 5th August) in Italy. The SW USA had also a very hot summer, with Death Valley recording the highest July mean temperature (41.9 °C) in USA on record. Record-high temperatures occurred also in California in September (41.1 °C in San Francisco) (WMO, 2018).

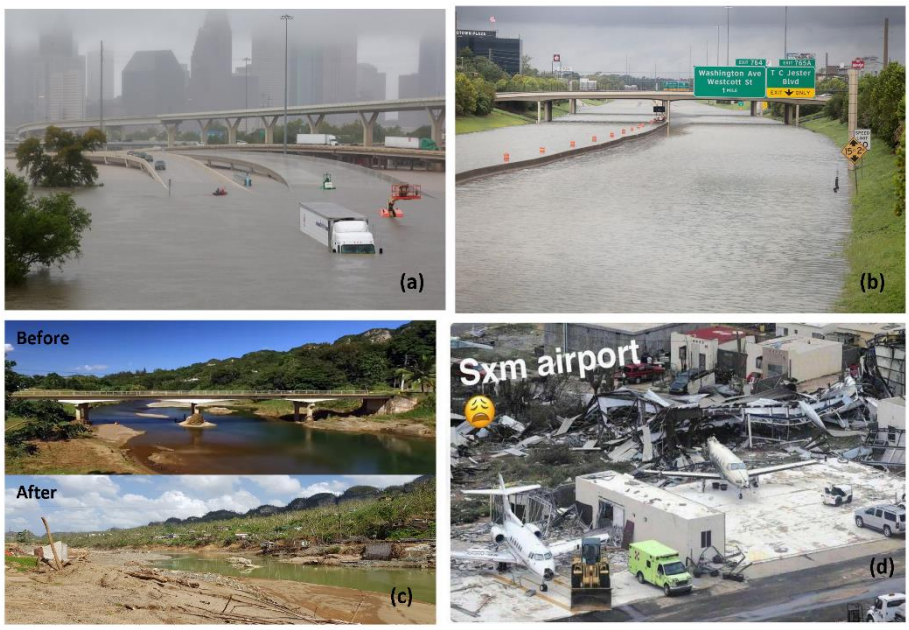

Figure 14 *Transport infrastructure damages from the 2017 hurricanes. (a) Harvey: highway flooding in downtown Houston (USA) (https://www.pbs.org/newshour/science/hurricane-harvey-became-extreme). (b) Harvey: Houston highways (https://www.vox.com/science-and-health/2017/8/28/16211392/100-500-year-flood-meaning). (c) Maria: Bridge at Puerto Rico) (https://coastalresiliencecenter.unc.edu/2018/10/lessons-learned-from-hurricanes-irma-and-maria/). (d) Distraction of the Sintt Maarten Princess Juliana international airport by Hurricane Irma (September 2017) (https://sxmgovernment.com/2017/09/07/new-photos-hurricane-irmas-destruction-of-st-maartens-princess-juliana-international-airport/)*

N. America experienced severe droughts in 2012 and 2013. In July 2012, 64.5 % of the US territory was classified as experiencing droughts, the largest areal extent since the 1930s. Total rainfall in 2011 - 2016 was 30 % below normal, resulting in economic losses of about US$60 billion. Long-term droughts also occurred in Australia and southern Africa, whereas the Indian monsoon rainfall (June-September) was about 10 % below normal in both 2014 and 2015 (WMO, 2016). In 2017, many Mediterranean areas experienced severe droughts, as did parts of central Europe. Italy had its driest January - August period on record (rainfall 26 % below the 1961–1990 average), Spain had its driest autumn on record and Portugal its third driest year on record. Eastern Mediterranean was also badly affected, including eastern Turkey, Cyprus and Israel. There were also severe droughts in North America. The 2016 - 2017 winter brought heavy rainfall to California after a prolonged drought; however, dry conditions resumed in the second half of the year (WMO, 2017; 2018). Regarding wildfires, 2017 was an active year, particularly for Portugal and NW Spain, Croatia, France and Italy and the western North America. Total economic losses for the 2017 California wildfires were assessed as US$ 18 billion, with the total area burnt in the contiguous USA being 53 % above the 2007−2016 average, just short of the 2015 record (WMO, 2015; 2018).

In 2012 - 2015, high wind and tornado activity in the USA was below the 1991-2010 average, but Europe encountered several extra-tropical cyclone-associated windstorms. In 2013, Denmark experienced

extreme winds (53.5 m/s) that caused excessive damage. The highest storm surge levels since 1953 were recorded in Netherlands and the UK. In the UK, the 2013 - 2014 winter was the wettest on record and there were also severe wind damage and coastal erosion (WMO, 2016). In 2016, tornado activity in the USA was below its long-term average (985 tornadoes, 10 % less than the post-1990 average). There were, however, thunderstorms, with hailstorms resulting in damages in excess of US$5 billion in Texas (WMO, 2017; NSIDC, 2017). In 2017, central and eastern Europe also suffered severe thunderstorms. Winds, exceeding 100 km/h resulted in widespread damage (and at least 11 deaths) in Moscow (29th May 2017). Noteworthy windstorms also occurred in Innsbruck, Austria (165 km/h wind gusts, 30th July) and in southern Finland (12th August). 2017 showed an above-average tornado season in the USA (1406 tornadoes, 12 % above the 1991–2010 average). A severe windstorm (*Zeus*) affected France in early March (gusts of 193 km/h in Brittany), whereas strong windstorms also occurred in Austria and the Czech Republic in late October, with gusts exceeding 170 km/h (WMO, 2018).

1.1.6 Forcing Mechanism

A major cause of the observed increase of the heat content of the planet is considered to be the increasing concentrations of atmospheric Greenhouse Gases (GHGs) that enhance the "greenhouse effect", a well documented and understood physical process of the Earth System since the 19th century (e.g. Canadell et al., 2007). GHGs absorb heat reflected back from the Earth's surface and, thus, store more heat in the ocean, land and atmosphere (IPCC, 2013). Without the greenhouse effect, the average temperature on Earth would be about -19 °C, i.e. about 34 °C colder than it is at present. All planets with heat absorbing gases in their atmosphere, experience a greenhouse effect. For example, the extreme hot surface temperatures of Venus are due to the high concentration of GHGs in its atmosphere.

Water vapor, an abundant GHG, makes the greatest contribution. The ability of the atmosphere to retain water vapor increases with global warming; thus, water vapor not only follows, but exacerbates changes in global temperature induced by the increasing concentrations of the other GHGs (e.g. Richardson et al., 2009; Shakun et al., 2012). The atmospheric concentrations of CO2, CH4 and the other GHGs have increased very substantially over recent decades (Fig. 15), probably as a result of human activities (IPCC, 2013).

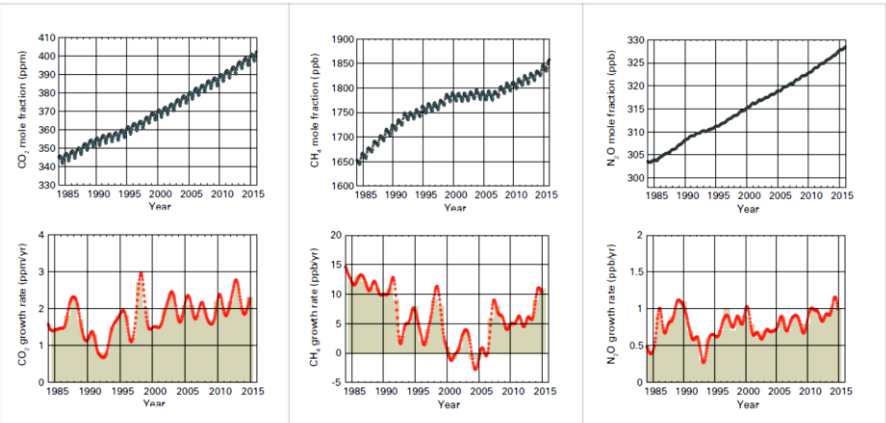

Figure 15 *Top row: Globally averaged mole fraction (measure of concentration) from 1984 to 2016, of CO2 in parts per million (left), CH4 in parts per billion (middle) and N2O in parts per billion (right). Bottom row: The growth rates representing increases in successive annual means of mole fractions for CO2 (left), CH4 (middle) and N2O (right) (WMO, 2018).*

Measurements of CO2 in the atmosphere and in ice-trapped air show that GHGs have increased by about 40 % since 1800, with most of the increase occurring since the 1970s when global energy consumption accelerated (EEA, 2015a). Ice core data suggest that current CO2 concentrations are higher than at any time in the last 2 million years years (Fig. 16), with the 400 ppm milestone reached in 09/05/2013 (NOAA, 2015).

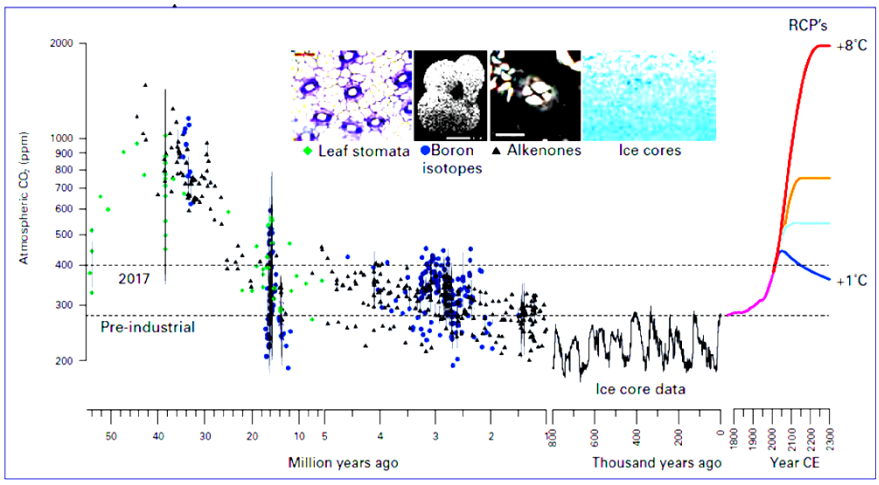

Figure 16 *Reconstruction of atmospheric CO2 over the past 55 million years based on proxy data (boron isotopes-blue circles, alkenones-black triangles and leaf stomata-green diamonds). Direct measurements from the past 800,000 years from Antarctic ice cores and modern instruments-pink. Future estimates are for the IPCC Representative Concentration Pathways (RCPs) 8.5 (red), 6 (orange), 4.5 (light blue) and 2.6 blue [6]. Key: CE, Current Era (WMO, 2018).*

Despite some climate mitigation measures, total global GHG emissions have increased continuously in recent decades (Figs. 15 and 16). Since 2014, CO_2 and N_2O concentration had growth rates slightly higher than the 1995-2014 average. CH_4 concentration also showed growth, following a period of little change in 1999-2006 (NOAA, 2015; WMO, 2016). It has been estimated that approximately 44 % of the total CO_2 emitted by human activities may remain in the atmosphere, with the remaining 56 % stored in the oceans and the terrestrial biosphere (WMO, 2014, 2016). In addition, there appears to be a good correlation between the CO2 concentration and heat storage in the ocean (Fig. 17), which also presents an increasing problem for the coastal communities and infrastructure due to the documented relationship between ocean heat storage and SLR (see also Fig. 5).

[6] Since the last IPCC Assessment Report AR5 (2013) forecasts are made on the basis of the Representative Concentration Pathways-RCP scenarios and not the IPCC SRES scenarios. The CO2 equivalent concentrations have been set to: RCP 8.5, 1370 C02-equivalent in 2100; RCP 6.0 850 CO2-equivalent in 2100; RCP 4.5, 650 CO2-equivalent in 2100; and RCP 2.6, peak at 490 CO2-equivalent before 2100 (Moss et al., 2010).

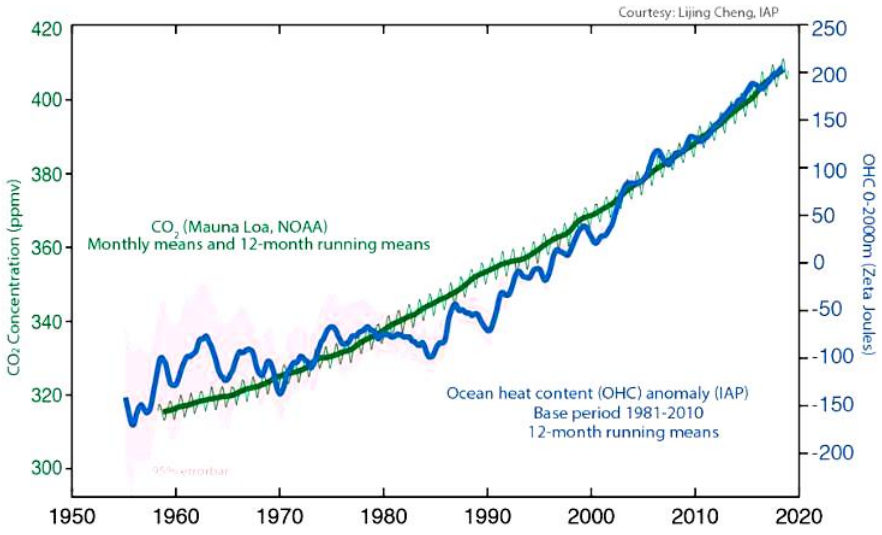

Figure 17 *Evolution of ocean heat content (to 2000 m depth) and of the atmospheric carbon dioxide concentration (Source L. Cheng).*

Breakdown of the total anthropogenic GHG emissions for 2010 revealed that CO2 accounted for 76 % (65 % due to fossil fuel combustion/industry and 11% due to land-use), CH4 for 16 %, N2O for 6 % and fluorinated gases for 2% of the emissions (IPCC, 2014). Analysis of the total CO2 emissions from combustion for the period 1971–2010 showed that the primary drivers of the increasing trend are population growth and patterns of consumption/production (IPCC, 2014). Assessment of the CO2 emissions in relation to country income shows that these doubled for upper-mid-income countries (e.g. China and South Africa) for the period 1990-2010, almost reaching the level of high income countries (Fig. 18). A notable increase of CO2 emissions was also found in lower-mid-income countries (IPCC, 2014).

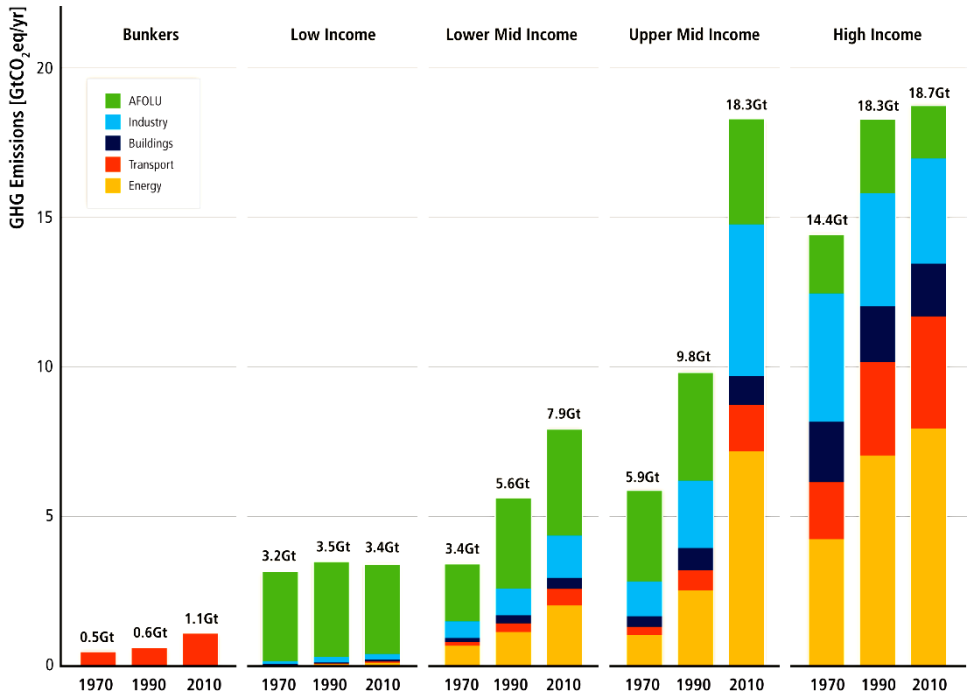

Figure 18 *Total anthropogenic GHGs in 1970, 1990 and 2010 by economic sector and country income groups (IPCC, 2014)*

1.2 Recent Climate Projections

The now better recorded/understood climatic factor dynamics (e.g. temperature, sea level and cryosphere) suggest a substantial and, in some cases, accelerating climatic change. This information suggest that transport-affecting climatic hazards (ECE, 2013) are 'deteriorating'.

Projections for the end of the 21st century indicate that atmospheric temperature will increase between 1.0 and 3.7 °C (mean estimates, Table 1), depending on the scenario. Forced by a range of possible Greenhouse Gas (GHG) concentration scenarios (IPCC, 2013), the central (mean) estimate for the warming has been predicted to be 1.0 - 2.0 °C for the period 2046 – 2065 compared to the mean of the period 1986 – 2005, whereas by the late 21st century (2081 – 100) increases of 1.0 - 3.7 °C are projected. However, the range of the projections broadens to 0.3 - 4.8 °C when model uncertainty is included.

The ocean will also warm. The strongest surface warming is projected for the subtropics and tropics, whereas warming at greater depths will be more pronounced in the Southern Ocean. Warming of the upper 100 m of the ocean has been estimated from 0.6 °C (RCP2.6) to 2.0 °C (RCP8.5), and for the upper 1,000 m from 0.3 °C (RCP2.6) to 0.6 °C (RCP8.5) at the end of the century. For RCP4.5, half of the energy taken up by the ocean has been projected to be stored in the uppermost 700 m and 85 % in the uppermost 2000 m (e.g. Cheng et al., 2019a; 2019b). Due to the long time scale of the heat transfer from the surface to deeper waters, warming will continue for centuries (IPCC, 2013).

Table 1 *Forecasts of global mean surface temperature and global mean sea level changes for the period 2081-2100 (means and likely ranges) with respect to the period 1986–2005, according to different RCP scenarios (IPCC, 2013).*

Scenario	Temperature		Sea Level Rise	
	Mean (°C)	Likely Range (°C)	Mean (m)	Likely Range (m)
RCP 2.6	1.0	0.3-1.7	0.40	0.26-0.55
RCP 4.5	1.8	1.1-2.6	0.47	0.32-0.63
RCP 6.0	2.2	1.4-3.1	0.48	0.33-0.63
RCP 8.5	3.7	2.6-4.8	0.63	0.45-0.82

The most recent IPPC assessment (IPCC, 2018) projects significant regional differences in climate characteristics between present-day and global warming of 1.5°C, and between 1.5°C and 2°C. These include increases in: mean temperature over most the land and ocean (high confidence), hot extremes in most inhabited regions (high confidence), heavy precipitation in several regions (medium confidence), and droughts and precipitation deficits in some regions (medium confidence).

1.2.1 Temperature and Precipitation

Climate does not and will not change uniformly, with temperatures close to the poles rising faster than at the equator (Figs. 3, 11 and 19). Precipitation is changing in a much more complex manner, with some regions becoming wetter and others dryer (ECE, 2013). Such trends are expected to pick up pace in the future. Under both the moderate (RCP4.5) and 'business as usual' emission (RCP8.5) scenarios, large increases in temperatures have been projected, particularly for the northern UNECE region (Fig. 19).

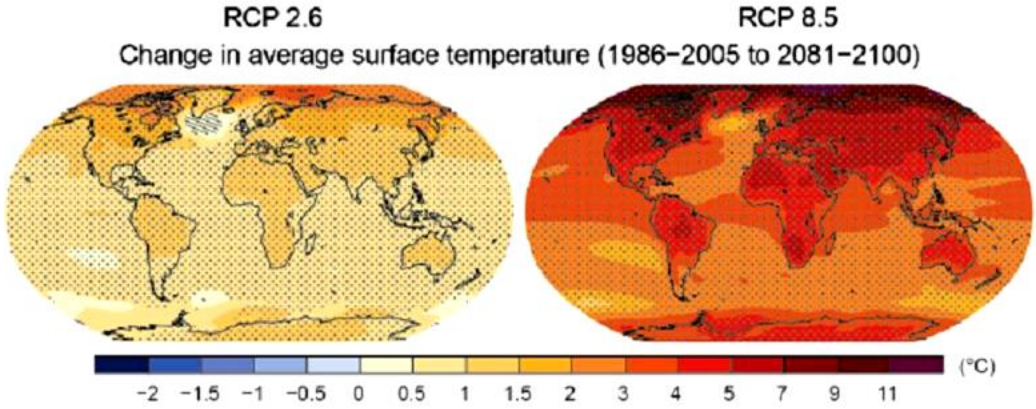

Figure 19 *Projected changes in average temperatures in 2081-2100 relative to 1986-2005 for low (RCP2.6) and high emission (RCP8.5) scenarios (IPCC, 2013).*

Regional models also suggest very significant warming for Europe (Fig. 21), which will be much more severe under RCP8.5. Northeastern Europe as well as the Mediterranean region will be the worst hit, with significant implications for the e.g. the UNECE rail network.

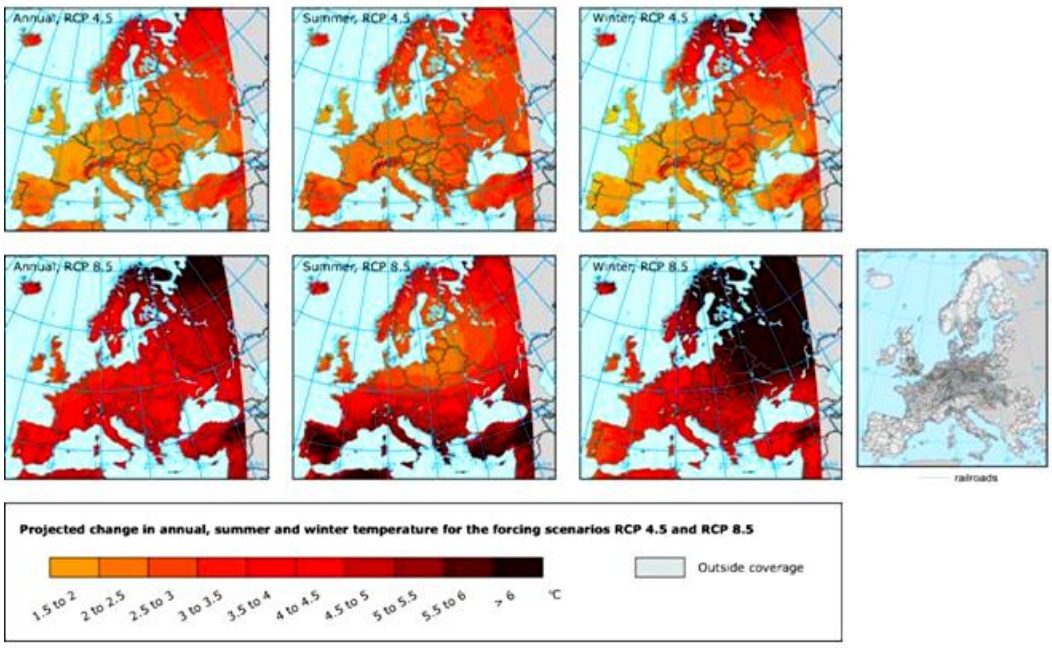

Figure 20 *Projected changes in annual (left), summer (middle) and winter (right) surface air temperature (°C) in 2071 - 2100 compared to 1971 - 2000 for forcing scenarios RCP4.5 (top) and RCP8.5 (bottom). Model simulations are from RCMs (EURO-CORDEX initiative) (EEA, 2014a).*

Regarding temperature variability, Vogel et al. (2017) have found that the multimode mean of daily maximum temperature (TX_X) increases globally in simulations (CTL and SM20c models) until the end of the century. Projected changes are more pronounced in CTL simulations, with regional increases of up to 10 °C, whereas in SM20c simulations temperature changes vary between 1°C and 6°C (Fig. 21, top).

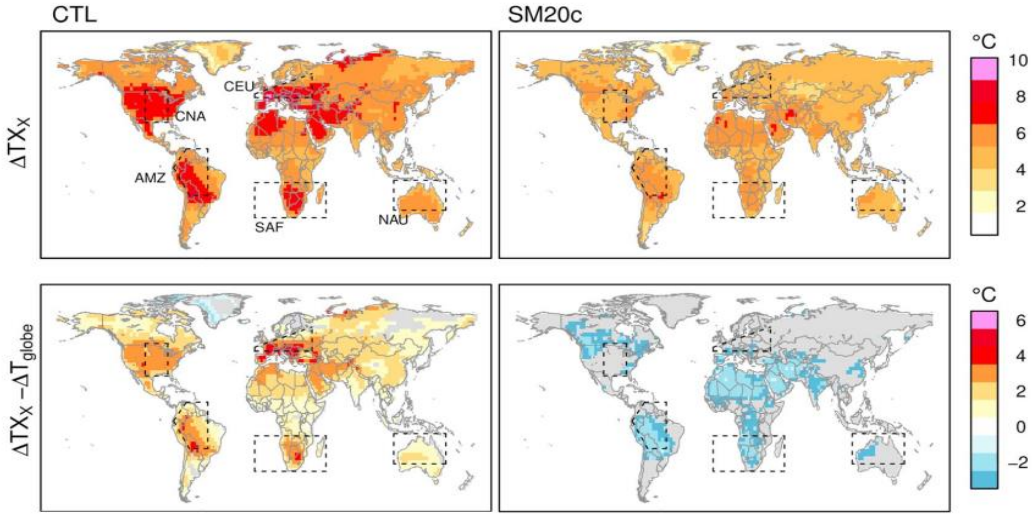

Figure 21 *Projected changes in daily maximum temperature TX_X (top row) between 2081 – 2100 and 1951 – 1970 and additional increase of TX_X versus Tglobe (bottom row) between 2081 – 2100 and 1951 – 1970 for CTL (left) and SM20c (right) simulations. Grey color denotes model disagreement (Vogel et al., 2017).*

There also appear to be large regional differences between the projected TX_X increase in Central Europe, Central North America, Northern Australia and Southern Africa. Such differences may indicate soil moisture feedbacks for extreme temperatures in these regions (Vogel et al. (2017).

Changes in precipitation patterns are projected for the UNECE region, with the north becoming wetter and the south drier (Fig. 22). Widespread droughts across most of southwestern North America and other subtropical regions are projected for the mid to late 21st century (Milly et al., 2008; IPCC, 2013). By comparison, while summers are expected to become (overall) drier by 2100 over the UK (see e.g. Fig. 22), downpours may become heavier; simulations indicate that intense downpours which are associated with flash flooding (> 30 mm in an hour) could become almost 5 times more frequent (MetOffice, 2014).

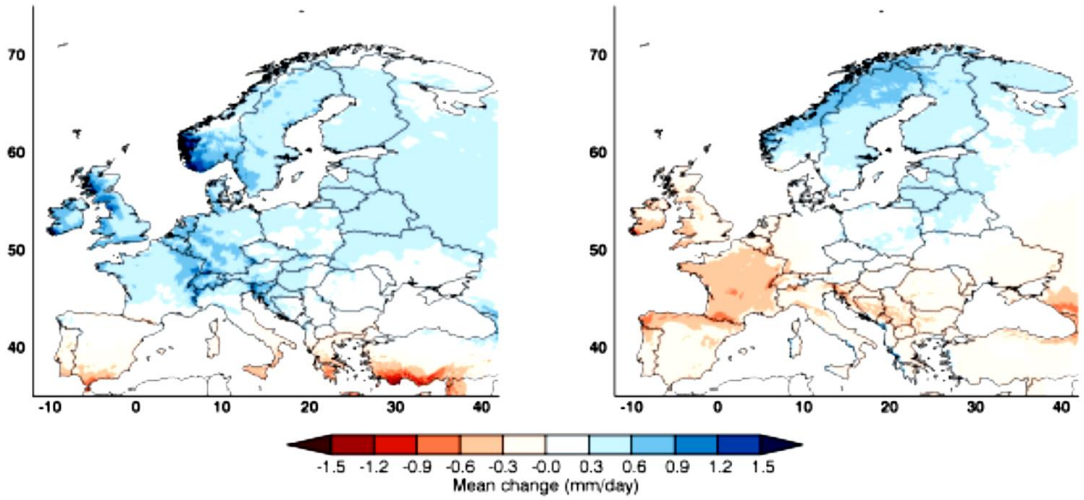

Figure 22 *Projected change of daily precipitation in winter (left) and summer (right), at the end of the century (2071-2100) compared to the present climate (1981-2010), under RCP8.5.*

Studies also project decreases in the duration/intensity of droughts in the South Europe and the Mediterranean, the central Europe and parts of the North America (e.g. IPCC, 2013). At the same time, studies suggest severe/widespread droughts for the next 30 – 90 years (Dai, 2013) for most of southwestern North America and the subtropical regions (IPCC, 2013; 2018).

1.2.2 Arctic ice, snow and permafrost

Snowfall and rainfall are projected to increase in the Arctic regions. Winter snow depth is projected to increase over many areas, with the most substantial increase (15 to 30 % by 2050) taking place in Siberia. However, snow will tend to stand for 10 to 20 % less time each year over most of the Arctic, due to earlier spring melting (AMAP, 2012). Spring snow cover extent (SCE) in the North Hemisphere (NH) is projected to decrease by about 25 % (RCP8.5), by 2100 (Fig. 23). As for mountain glaciers and ice caps, climate model projections also indicate a 10 to 30 % mass reduction by the end of the century (AMAP, 2012).

Permafrost thawing is projected due to rising global temperatures and changes in snow cover (e.g. AMAP, 2012). Current warming rates at the European permafrost surface are 0.04 – 0.07 $^0C\ yr^{-1}$ (EEA, 2015a). Although there are challenges in assessing the permafrost change, including those related to soil processes, climate forcing scenarios and model physics, permafrost extent is expected to decrease by 37 %

and 81 % for RCP2.6 and RCP8.5 scenarios, respectively, by the end of the 21st century (medium confidence) (Fig. 23). Such changes could impose substantial problems in the development and maintenance of infrastructure in the Arctic region (ECE, 2013), that could constrain the development of transport networks to take advantage of the new Arctic Ocean routes made possible by the projected Arctic sea ice melt.

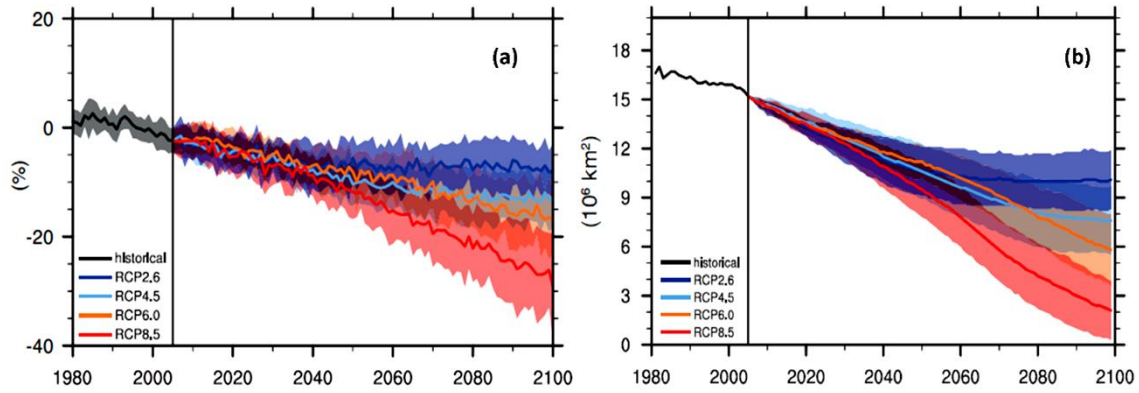

Figure 22 *Projected (a) snow cover extent (SCE) and (b) near-surface permafrost changes for 4 Representative Concentration Pathways-RCPs (CMIP5 model ensemble) (IPCC, 2013).*

It is likely that the Arctic sea ice will continue to decrease in extent/thickness as global mean surface temperature rises, although there will be considerable inter-annual variability. Based on the CMIP5 model ensemble, Arctic sea ice extent (SIE) is projected to decrease considerably. In 2081 - 2100, reductions of 8 to 34 % in February and of 43 to 94 % in September are projected compared to the average SIE in 1986 – 2005 (the low and high projections refer to the RCP2.6 and RCP8.5, respectively) (IPCC, 2013).

Global warming will have a strong impact on the Greenland Ice Sheet (GIS) in the following decades, the Surface Mass Balance (SMB) of which has shown a decreasing trend recently (Velicogna et al., 2014; Hansen et al., 2016). Based on the available evidence, however, it is unlikely that SMB changes will result in a collapse of the GIS in the current century. IPCC (2013) has suggested that the dynamical change of GIS in this century could contribute to SLR by 20 to 85 mm (RCP8.5), and 14 to 63 mm for all other scenarios (medium confidence). Other studies project SMBs changes of 0.92 ± 0.26 mm yr^{-1} (compared to the 1961 – 1990) (Hansen et al., 2016). By comparison, the SMB of the Antarctic ice sheet has been projected to increase under most scenarios due to an increasing snowfall trend (but see the recent observations of Rignot et al. (2019)). In any case it should be noted that potential negative Antarctica SMBs might contribute more than 1 m of SLR by 2100 (De Conto and Pollard, 2016).

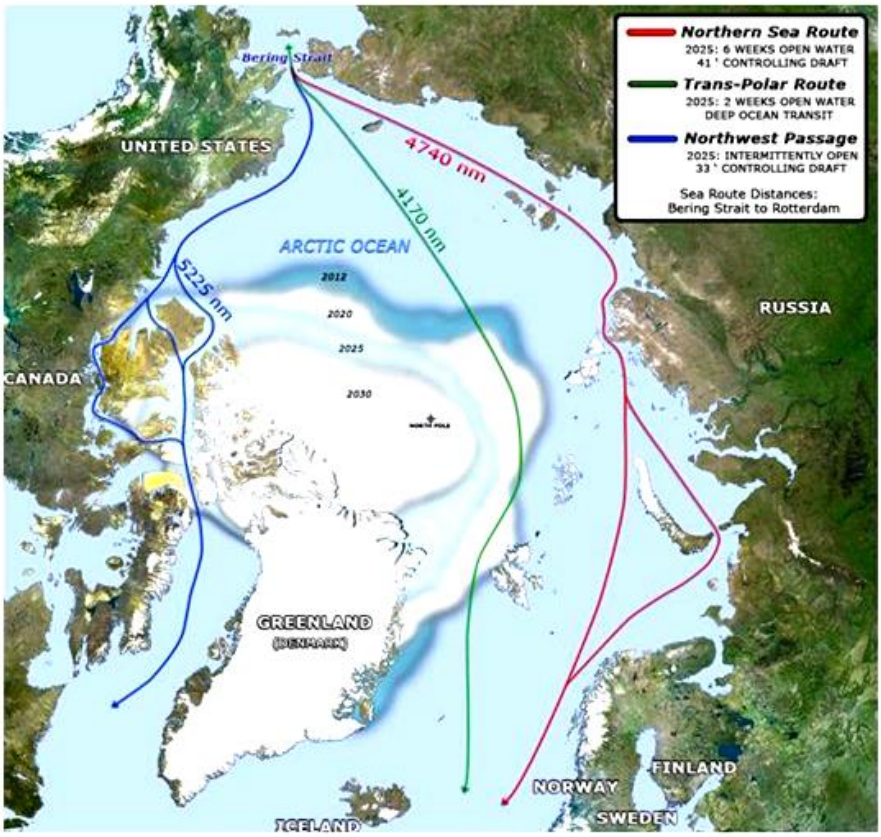

Figure 23 *New Arctic shipping routes (U.S. Climate Resilience Toolkit, 2015).*

There may be new socio-economic opportunities for Arctic communities, as the reducing SIE facilitates access to the substantial natural resources such as the hydrocarbon deposits at Beaufort and Chukchi seas and promotes Arctic international shipping trade. The US Navy anticipates the development of 3 major shipping routes by 2025 (Fig. 23) in the Arctic Ocean. In Russian Federation, several seaports have been already developed (Fig. 24) to service commodity transportation. In 2017, the cargo turnover in these seaports has increased by 1.5 times compared to 2016, reaching 73 million tons; by 2030, the turnover is expected to increase further to 140 million tons (S. Egorshev, 2018)[7].

There are, however, environmental risks and development challenges associated with the exploitation of the new Arctic routes. CV & C will affect existing and future infrastructure due e.g. to thawing permafrost and coastal wave activity (see below), that will require specialized and innovative adaptation measures (S. Egorshev, 2018)[8].

[7]http://www.unece.org/fileadmin/DAM/trans/doc/2018/wp5/2_Russian_Federation_Mr_Egorshev_Climate_Change_18-19_December_2018.pdf

[8]For further information see the link at the footnote above.

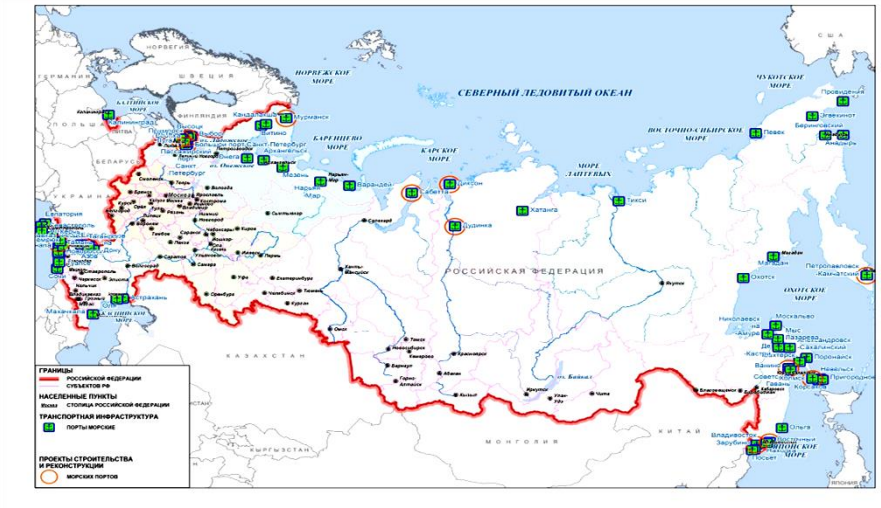

Figure 24 *Russian Federation Arctic seaports (S. Egorshev, 2018).*

1.2.3 Sea level and waves

Process-based predictions of the mean sea level rise (SLR) are constrained by uncertainties on the response to global warming and the variability of: the GIS and AIS mass balance (Pritchard et al., 2012; Hansen et al., 2016; Rignot et al., 2019); the steric changes (Domingues et al., 2008; Cheng et al., 2019a; 2019b); the contributions from mountain glaciers (Raper and Braithwaite, 2009; Menounos et al., 2018); and the groundwater pumping for irrigation purposes and the storage of water in reservoirs (Wada et al., 2012).

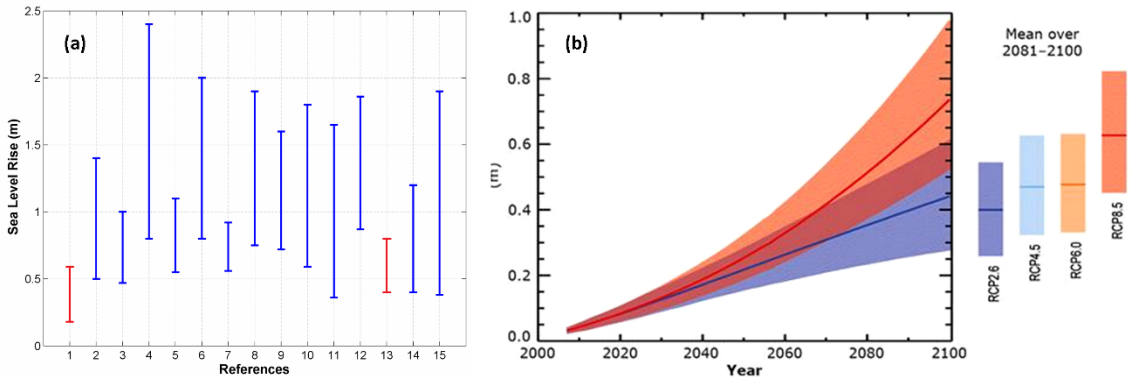

Figure 25 *(a) Recent sea level rise projections for 2100 compared to that of IPCC (2007a) and (2013). Key: 1, IPCC (2007a), 0.18-0.59 m; 2, Rahmstorf et al. (2007); 3, Horton et al. (2008); 4, Rohling et al. (2008); 5, Vellinga et al. (2008); 6, Pfeffer et al. (2008); 7, Kopp et al. (2009); 8, Vermeer and Rahmstorf (2009); 9, Grinsted et al. (2010); 10, Jevrejeva et al. (2010); 11, Jevrejeva et al. (2012); 12, Mori et al. (2013); 13, IPCC (2013); 14, Horton et al., 2014; and 15, Dutton et al., 2015. The variability of the projections reflects differences in assumptions and approaches. (b) Projected global MSLR over the 21st century relative to 1986-2005* (IPCC, 2013).

Global mean sea level has risen by 0.19 m between 1901 and 2013 (average rate 1.7-1.8 mm yr^{-1}), whereas in the last two decades, the rate has accelerated to almost 3.3 mm yr^{-1}. It is thought that the steepening of the curve of the SLR in recent decades is mostly due to the increasing contribution of ice mass loss from the Greenland-GIS and Antarctic ice sheets-AIS (e.g. Rignot et al., 2011; Hanna et al., 2013). Models project rises in 2081 – 2100 (compared to 1986 – 2005) of 0.26 – 0.54 m (RCP2.6) and 0.45 – 0.82 m (RCP8.5). Sea level estimates based on alternative approaches project increasingly higher SLRs than those predicted earlier (in IPCC (2007)). Here it should be noted that the IPPC has consistently provided conservative estimates (Fig. 25). SLR will continue beyond 2100 (Jevrejeva et al., 2012; 2016) (Fig. 26); increasing ocean heat content (e.g. Cheng et al., 2019a) will induce increasing thermal (steric) expansion for (at least) several centuries, whereas dynamic ice loss in Antarctica and Greenland will also continue well into the future.

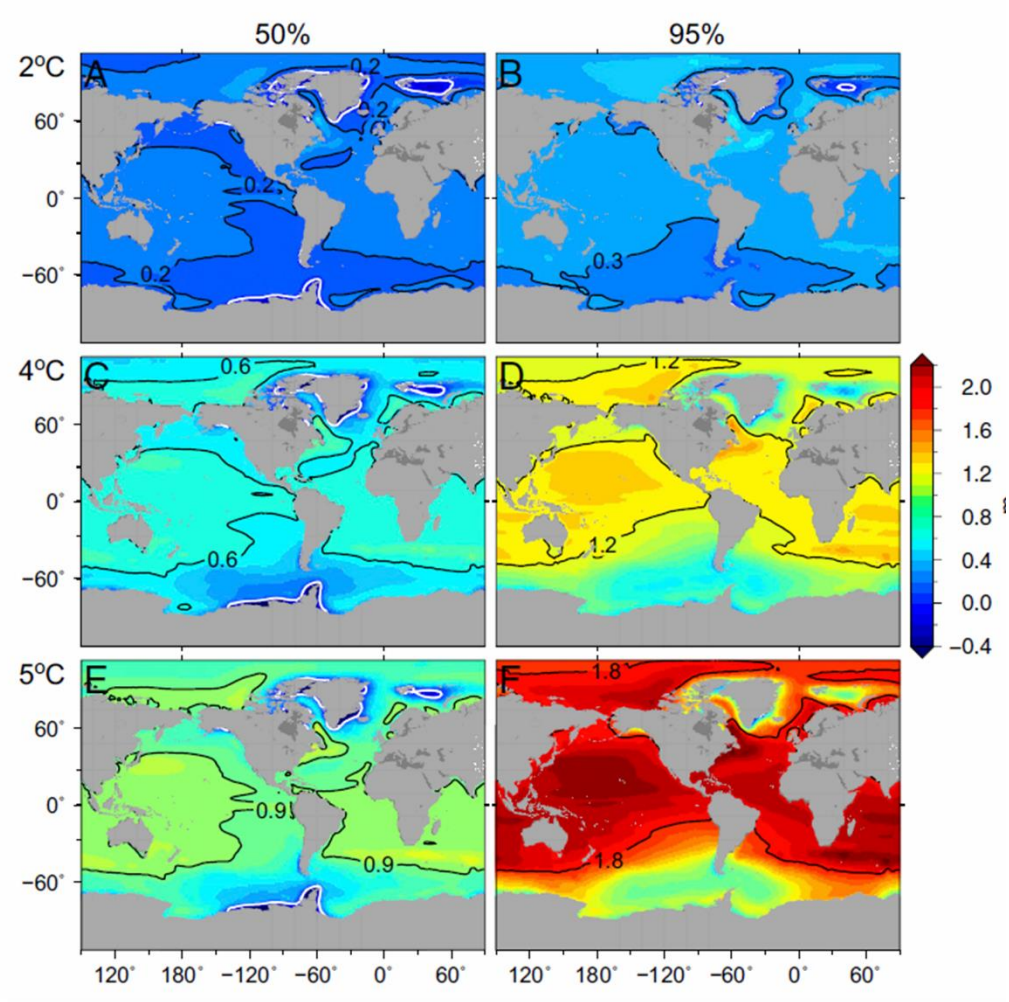

Figure 26 *Regional sea level projections for warming under the business as usual scenario (RCP8.5): (A and B) 2 °C, (C and D) 4 °C, and (E and F) 5 °C relative to 1986–2005. A, C, and E show median (50 %) projections, and B, D, and F show upper limits (95 %) projections. Black contours mark global sea level value, and white contours correspond to zero sea level rise (Jevrejeva et al., 2016).*

Due to the large spatial variability observed (and projected) in SLR, regional trends should be considered when assessing potential impacts along any particular coast (e.g. Carson et al., 2016). In addition to the global processes, regional factors can contribute to coastal sea level changes, such as changes in ocean circulation (e.g. Meridional Overturning Circulation-MOC), differential rates in regional glacial melting, glacio-isostatic adjustment (GIA) and coastal sediment subsidence (IPCC, 2013; King et al., 2015; Carson et al., 2016; Jevrejeva et al., 2016).

It should be noted that 2 °C of global warming above the pre-industrial level (the goal of the 2015 Paris Agreement) has been widely suggested as a threshold beyond which climate change risks become unacceptably high (but see also IPCC (2018)). Without effective mitigation measures, however, this threshold is likely to be reached before 2050 (under the business as usual scenario RCP8.5). Probabilistic SLR projections with warming at and above the 2 °C show that more than 90 % of the global coastline will experience rises exceeding the global estimate of 0.2 m, with rises up to 0.4 m expected along the Atlantic coast of North America and Norway (Fig. 26). By comparison, under a 5 °C rise (the upper limit of temperature rise in 2100, see Table 1), SLR will reach 0.9 m (median), and 80 % of the coastline will exceed the global SLR at the 95th percentile upper limit of 1.8 m (Jevrejeva et al., 2016). Palaoclimatic, instrumental and modeling studies have shown that combinations of global and regional factors can cause relatively rapid SLR rates along particular coasts that can exceed the global rates (e.g. Cronin, 2012).

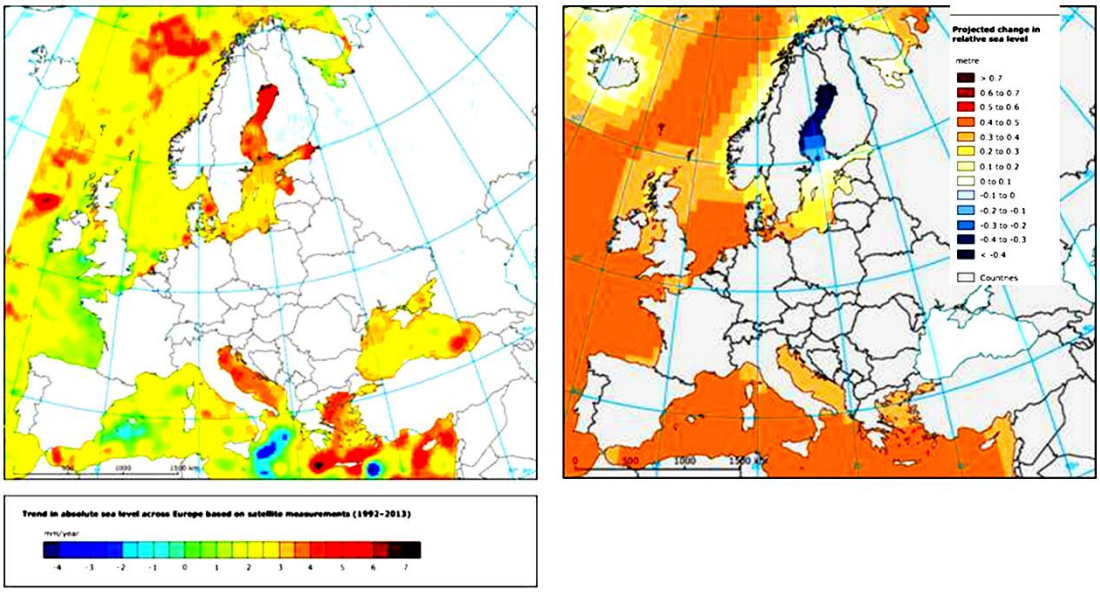

Figure 27 *Left: Trends in absolute sea level in European Seas from satellite measurements (1992–2013) (EEA, 2014b). Right: Projected change (CMIP5 ensemble) in relative sea level in 2081 - 2100 compared to 1986 - 2005 for the moderate emission scenario RCP4.5. No projections are available for the Black Sea (EEA, 2014c).*

In Europe, both the current trends and future projections suggest substantial regional SLR variability (Fig. 27). For the Netherlands coast, Katsman et al. (2011) have estimated sea level rises of 0.40 - 1.05 m for

a plausible high end emission scenario, whereas a SLR of up to 0.8 m has been projected for the Mediterranean region in 2100 (Hinkel et al., 2014; Jevrejeva et al., 2016).

In addition to SLR, CV & C impacts on coastal transport infrastructure/operations depend also on other factors/hazards, such the mean and extreme wave conditions and storm surges (see also Section 1.2.4). Camus et al (2017) have provided global multi-model projections of wave conditions (e.g. significant wave height[9]) under climate change (Fig. 28) to assist assessments on the impacts of CV & C on coastal transport infrastructure (see also Asariotis et al., 2017). Their results show consistent increases for the annual mean *Hs* for the Southern Ocean and eastern Pacific and consistent decreases for the North Atlantic, western North Pacific and Indian Oceans, with the magnitude of increases being about four times higher than the magnitude of the decreases. If these projections are combined with those of the SLR, then seaport operability can be assessed in view of the higher sensitivity of breakwaters with low freeboards (Camus et al., 2017).

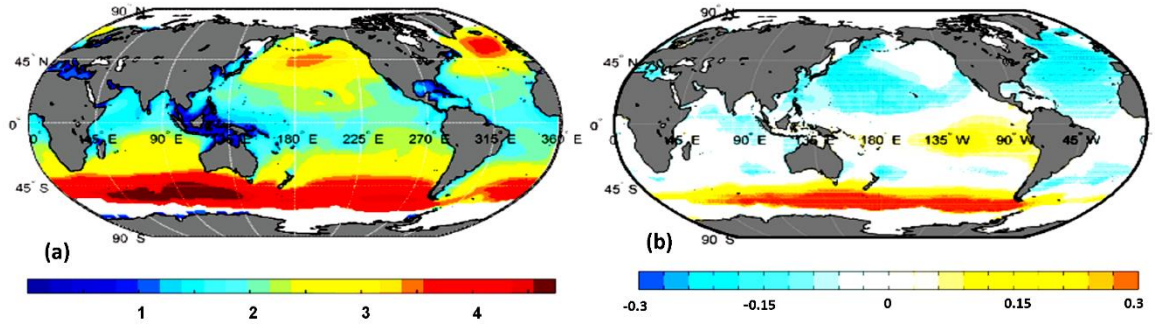

Figure 28 *(a) Multi-model annual mean significant wave height (m) for the time period 1979 – 2005. (b) Multi-model projected changes in annual mean significant wave height for 2070 – 2100 relative to 1979 – 2005 under RCP8.5. Stippling represents areas where the magnitude of the ensemble mean exceeds inter-model standard deviation (Camus et al., 2017).*

1.2.4 Extreme Events

Heat waves

Increases in hot extremes and decreases in cold winter extremes are expected by the end of the 21th century, with the frequency, duration and magnitude of the events being affected by anthropogenic forcing (IPCC, 2013). Greater changes in hot (seasonal) extremes are expected to take place in the subtropics and the mid-latitude regions (Fig. 30), whereas the frequency of cold events will decrease in all regions. Generally, very hot summers are projected to occur much more frequently in the future under all Climate Change scenarios.

[9] Annual significant wave height (Hs) is the mean of the highest one third of the waves recorded at a site in each year.

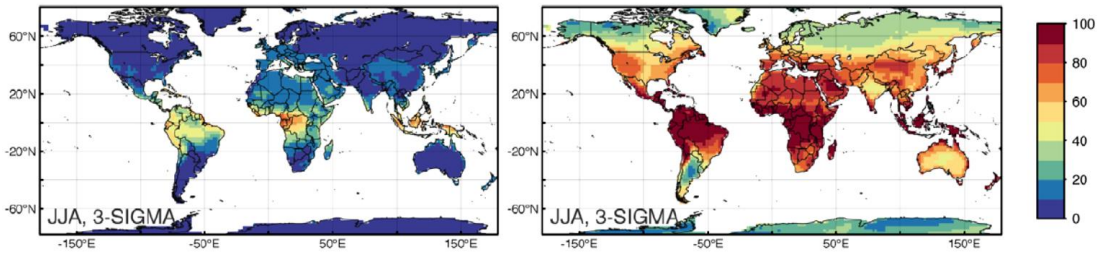

Figure 30 *Projected changes in hot seasonal temperature extremes in 2071 - 2100 for RCPs 2.6 and 8.5. Yellow, orange/red areas show regions where (at least) 1 every 2 summers will be warmer that the warmest summer in 1901 - 2100 (Coumou and Robinson, 2013)*

It is also likely that the frequency of heat waves (prolonged periods of excessive heat) in e.g. Europe will increase (Fig. 31), mainly due to the increasing seasonal summer temperatures. For most land regions it is likely that the frequency of a current 20-year hot event will be doubled (in many regions it might even occur every 1 - 2 years), while the occurrence of a current 20-year cold event will be reduced under the RCP8.5 scenario (IPCC, 2013). Large increases in heat waves are projected for the UNECE region under RCP8.5 (Figs. 30 and 31).

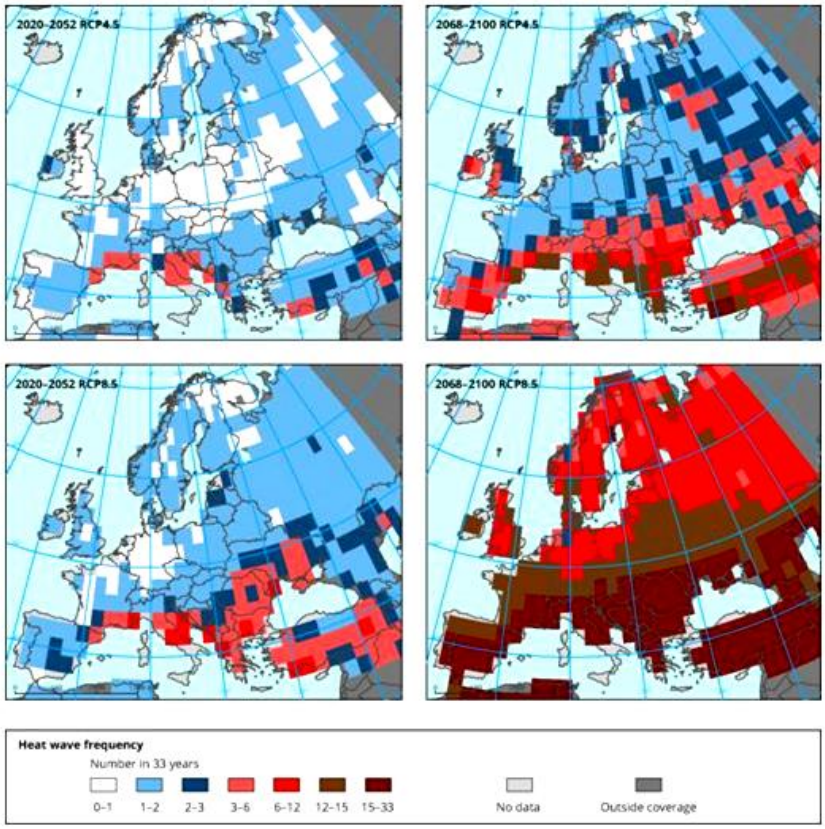

Figure 31 *Median of the projected number of heat waves (from a model ensemble) in the near (2020 – 2052) and long (2068 – 2100) term under the RCP4.5 and RCP 8.5 scenario (EEA, 2015b).*

Heat waves as severe as that of 2003 are expected to occur about once a century in the current climate; in early 2000s, such events were expected to take place approximately once every several thousand years. An attribution study has suggested that anthropogenic influence has at least doubled their probability of occurrence (MetOffice, 2014). Other studies suggest that the probability of occurrence of an extreme heat wave like that occurred in the Russian Federation in 2010 may increase by 5 - 10 times until 2050 (Dole et al., 2011).

As mentioned earlier (Section 1.1.4) the combination of extreme heat with high relative humidity-the Heat Index- may have very significant implications for the health/safety of personnel and passengers in most modes of transport. Projections (Mora et al., 2017) indicate substantial exceedance of the deadly threshold (Fig. 10) for the end of the century, which will be particularly severe under the business as usual scenario (RCP8.5), with direct impacts on southwestern USA and the Mediterranean UNECE region (Fig. 32).

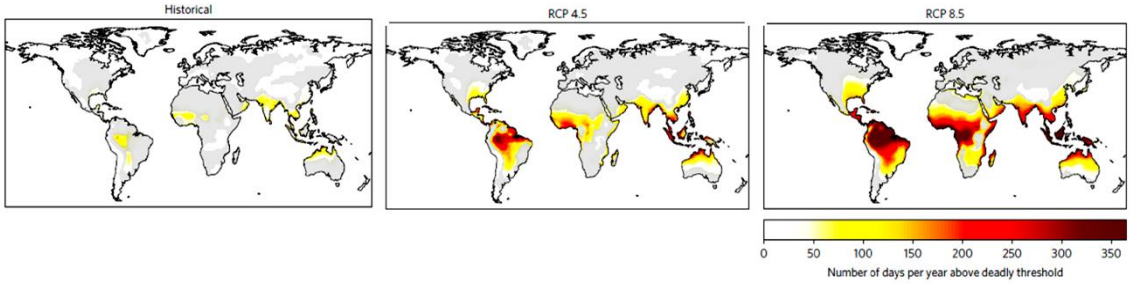

Figure 32 *Deadly climatic conditions in 2100 under different emission scenarios. Conditions refer to the number of days per year exceeding the threshold of temperature and humidity beyond which climatic conditions become deadly (see Fig. 10), averaged between 1995 and 2005 (historical experiment), and between 2090 and 2100 under RCP 4.5 and RCP 8.5. Results are based on multi-model medians. Grey areas indicate locations with high uncertainty (multi-model standard deviation larger than the projected mean) (Mora et al., 2017).*

Heavy precipitation (downpours)

Extremes linked to the water cycle, such as droughts, heavy rainfall and floods, are already causing substantial damages. As temperature rises, average precipitation will exhibit substantial spatial variation. It is likely that precipitation will increase in the high ad mid latitude lands and decrease in subtropical arid and semi-arid regions by the end of the century under the RCP8.5 scenario. Extreme precipitation events will be more intense over most of the mid-latitude and wet tropical regions (IPCC, 2013). For central and NE Europe, projections demonstrate large increases (25 %) in heavy precipitation by the end of the century (Fig. 33). High resolution climate models indicate that extreme summer rainfalls could intensify with climate change (MetOffice, 2014). For the UK, although summers will become drier overall, the occurrence of heavy summer downpours (more than 30 mm in an hour) could increase almost 5 times (MetOffice, 2014).

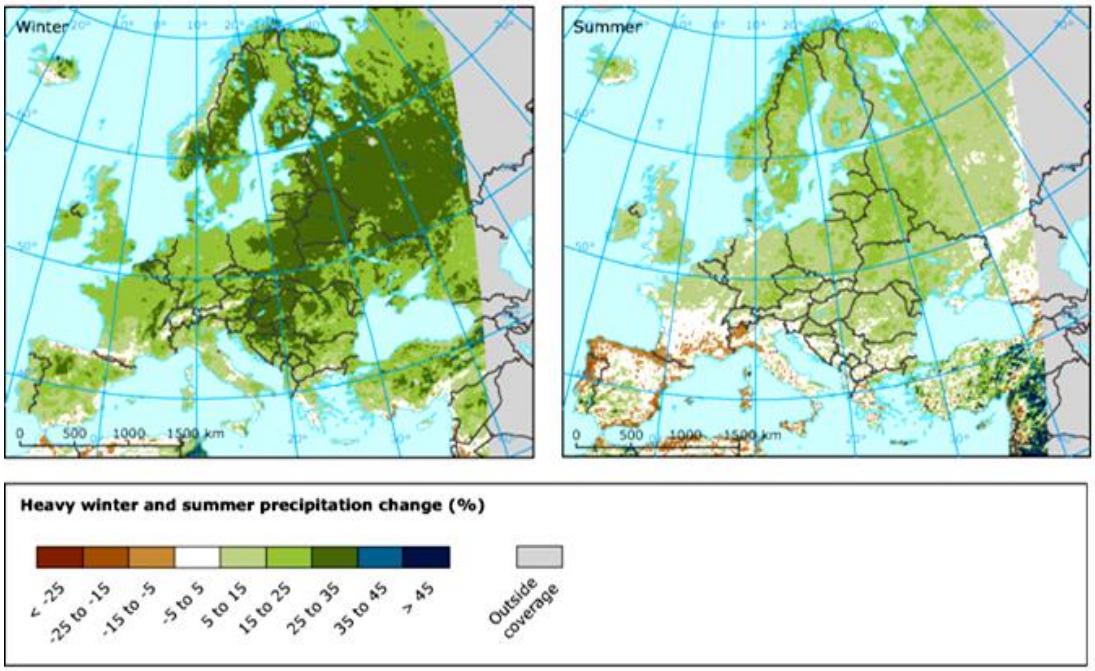

Figure 33 *Projected changes in heavy precipitation (in %) in winter and summer from 1971 - 2000 to 2071 – 2100 for the RCP8.5 scenario based on the ensemble mean of regional climate models (RCMs) nested in general circulation models (GCMs) (EEA, 2015c).*

Coastal sea storms and riverine floods

Despite the emerging risks associated with the changes in extreme coastal sea levels (ESLs), there is still limited information under the Representative Concentration Pathways (RCPs) (IPCC 2013). That's mainly because most previous studies have been at local/regional scale which implies that (a) there are several regions for which there is no information and (b) the use of different GHG emission scenarios, climate and ocean models, as well as the diversity of the coastal environments make it difficult to draw general conclusions at global or regional scales. Extreme coastal erosion and flooding are driven by the extreme waves and sea levels (e.g. Ranasinghe, 2016; Rueda et al., 2017), considered here as the sum of the mean sea level (*MSL*), the astronomical tide (η_{tide}) and the episodic coastal water level rise due to storm surges and wave set ups.

For Europe, projections show larger storm surge levels for the Atlantic and Baltic coast and ports under all scenarios and extreme storm events tested (Vousdoukas et al., 2016a; Vousdoukas et al., 2017). North Sea, an area subject to some of the highest SSLs in Europe, is projected to show an increase in the extremes, particularly along its eastern coast. Storm surges are projected also to increase along the Atlantic coast of the UK and Ireland, due mostly to a consistent increase in the winter extremes. Studies on the Mediterranean storm surge dynamics indicate small or no changes, with a decrease in the frequency and intensity of extreme events being likely (Conte and Lionello 2013; Androulidakis et al. 2015). This is in agreement with reported historical trends (Menéndez and Woodworth 2010), as well as with more recent findings which project changes mostly in the ±5 % band (Vousdoukas et al., 2016a). North Adriatic is a region which has been studied more thoroughly due to the highly vulnerable (and socio-economically

important) Venice area, with most projections reporting no statistically significant changes (Mel et al. 2013), although Lionello et al. (2012) projected increases in the frequency of extreme events around Venice under the B2 SRES scenario. In addition to storm surges energetic wave events will excacerbate the ESLs (Vousdoukas et al., 2018) as e.g. along the Atlantic coast of France, Spain and Portugal that are exposed to energetic waves (Pérez et al. 2014).

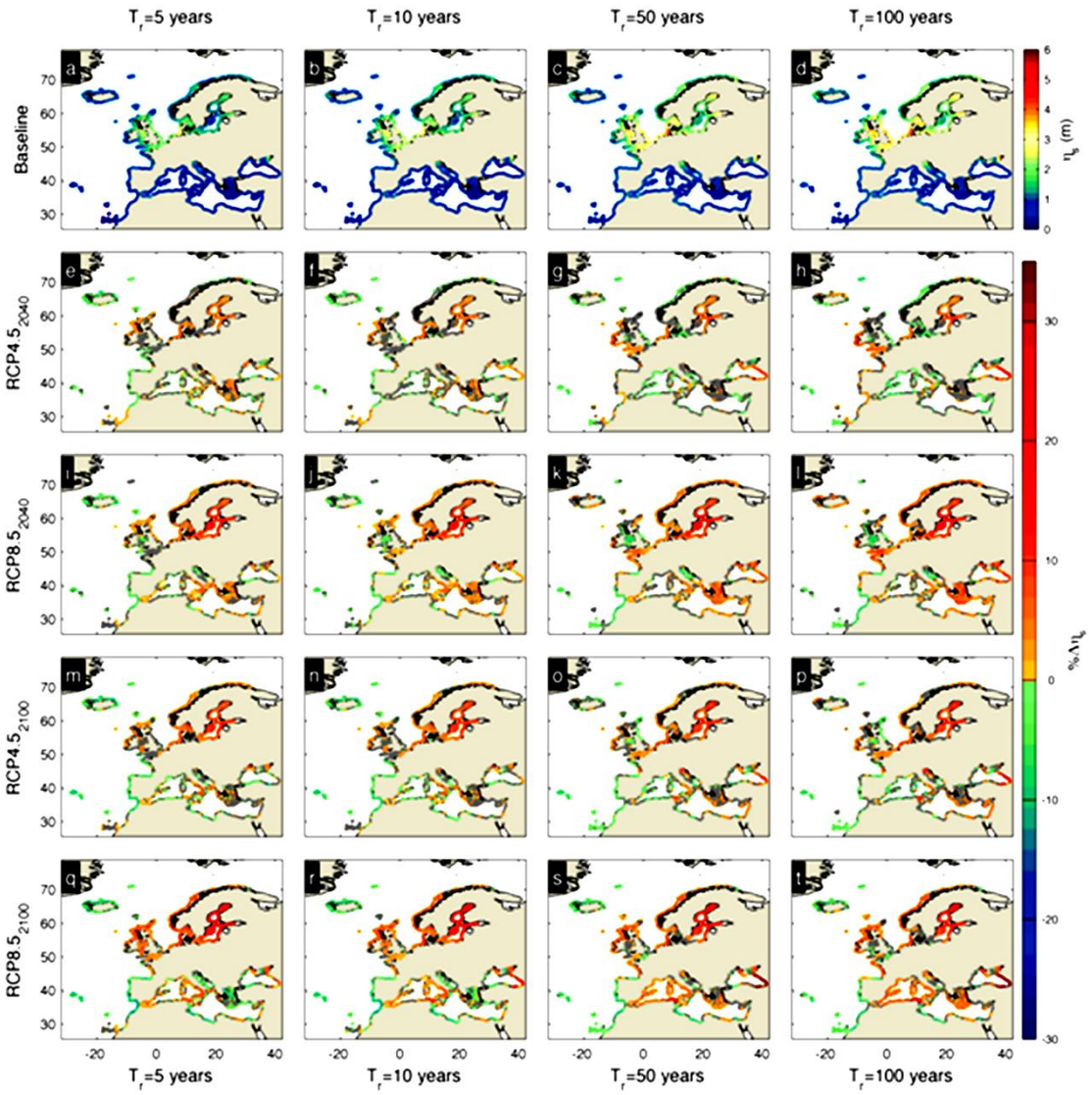

Figure 34 *Ensemble mean of extreme storm surge levels (m) along the European coastline obtained for 5, 10, 50, and 100 years return periods (shown in different columns), for the baseline period (a–d), as well as their projected relative changes in 2040 under RCP4.5 (e–h) and RCP8.5 (i – l) and in 2100 under RCP4.5 (m–p) and RCP8.5 (q–t). Warm/cold colors express increase/decrease, respectively; points with high model disagreement are shown with gray colors (Vousdoukas et al., 2016a).*

It should be noted that more than 200 million people worldwide live along coastlines with an elevation of less than 5 m above sea level; this figure is estimated to increase to 400 - 500 million by the end of the 21st century. Growing exposure (population and assets), rising sea levels due to CV & C, and in some

regions, significant coastal subsidence due to human coastal water drainage/groundwater withdrawals will increase the flood risk to varying degrees. For instance, a 1 m rise in relative sea level may increase the frequency of current 100 year flood events by about 40 times in Shanghai, about 200 times in New York, and about 1000 times in Kolkata (WMO, 2014).

For the next 50 years or so, Hallegatte et al. (2013) suggested that for the 136 largest coastal cities: (i) damages could rise from US$ 6 billion/year to US$ 52 billion/year due to increase in population and assets; (ii) annual losses could approach US$ 1 trillion or more per year if flood defenses are not upgraded; (iii) even if defenses would be upgraded, losses could increase as flood events could become more intense due to the SLR. This raises the question of whether there are potential thresholds which, if passed, could reverse the current and projected trends of coastal population growth (King et al., 2015). Taking into account the standards of coastal flood protection works and uncertainties concerning the probability of their failure, about 5 million people in Europe could potentially be affected by the present day 100-year extreme sea level-ESL_{100} (Vousdoukas et al., 2016b).

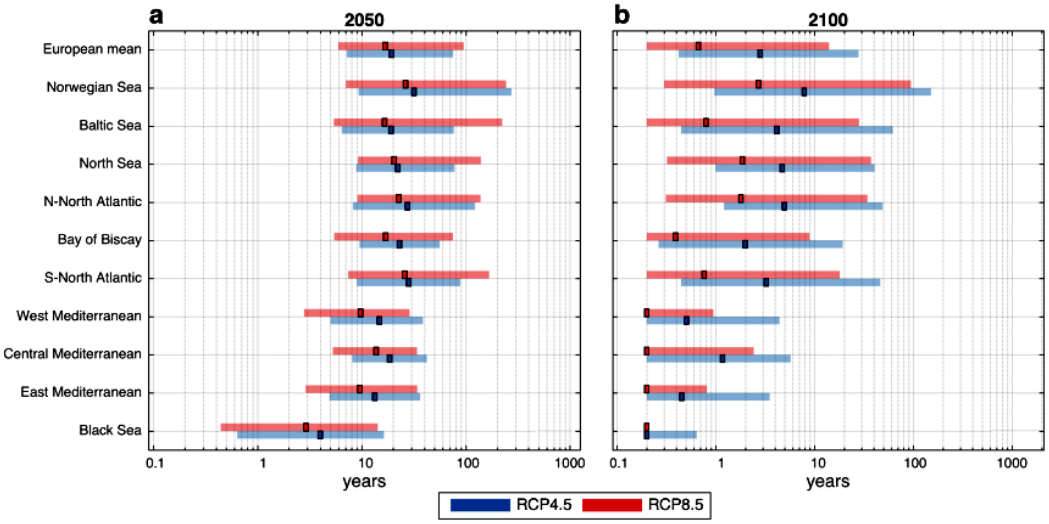

Figure 35 *Return period of the present day 100-year ESLs along the European coastline under RCP4.5 and RCP8.5 in 2050 (a) and 2100 (b). Colored boxes express the ensemble mean value and colored patches the inter-model variability (best-worst case (Vousdoukas et al., 2017).*

Averaged over Europe's coastlines, the present 100-year ESL (ESL_{100}) is projected to occur approximately every 11 years by 2050, and every 3 and 1 years by 2100 under RCP4.5 and RCP8.5, respectively (Fig. 35). Hence, the 5 million Europeans (and their transport infrastructure) currently at risk once every 100 years, may be flooded at an almost annual basis by the end of the century (Vousdoukas et al., 2017). Some regions are projected to experience an even higher increase in the frequency of occurrence of extreme events, most notably along the Mediterranean and the Black Sea, where the present day ESL_{100} is projected to occur even more often.

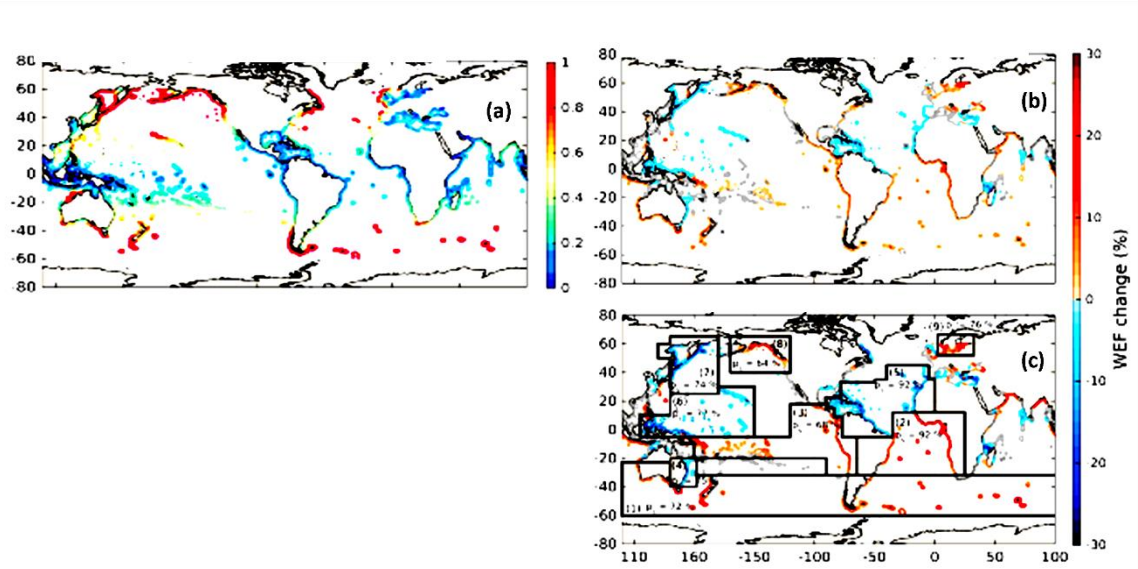

Figure 36 *Projections of wave energy flux-WEF along the global coastline: (a) baseline 100-year return level and relative change of the 100-year WEF for the year (b) 2050, and (c) 2100. Grey dots correspond to locations with no significant change. In (c), areas of significant change are reported together with the percentage ps of points where increase is significant. (1) Southern temperate zone, (2) S. Atlantic, (3) sub-equatorial-tropical E. Pacific, (4) E. Australia, (5) N. tropical Atlantic, (6) NW tropical Pacific, (7) NW Pacific, (8) NE Pacific, and (9) Baltic Sea (Mentaschi et al., 2017).*

For the end of the 21st century, recent modeling results under the business as usual scenario (RCP8.5) suggest an increase of up to 30 % in the 100 year return level of wave energy fluxes (WEF) for most coastal areas of the southern temperate zone, with the exception of Eastern Australia, the southern Atlantic, and the sub-equatorial-tropical E. Pacific (Mentaschi et al., 2017). By comparison, large coastal areas in the NH are projected to have a negative trend, with the exception of the NE Pacific and the Baltic Sea (Fig.36) which are projected to show positive trends (increases of up to 30 %).

Riverine flooding poses a most significant threat to transport infrastructure (ECE, 2013) as well as the global population. Increases in extreme runoffs have been well documented (Feyen et al., 2010), but the damage magnitude is mainly due to the increasing human and infrastructure exposure in the flood plains (IPCC, 2013). Changes in river floods projected for Europe are presented in Fig. 37).

Recent modeling results indicate that global warming is also linked to a substantial increase in riverine flood risk over most central and western Europe (no model agreement for eastern Europe). Alfieri et al. (2015) have estimated the expected riverine damage with a model super-ensemble that the € 7 billion/year damages of the 1976-2005 will increase to € 15 billion/year under a 1.5°C temperature increase since the pre-industrial times expected to occur in the early 2030s (IPCC, 2018). Damages from riverine floods are expected to be generally higher in the north than in the south (Alfieri et al., 2015; 2018)

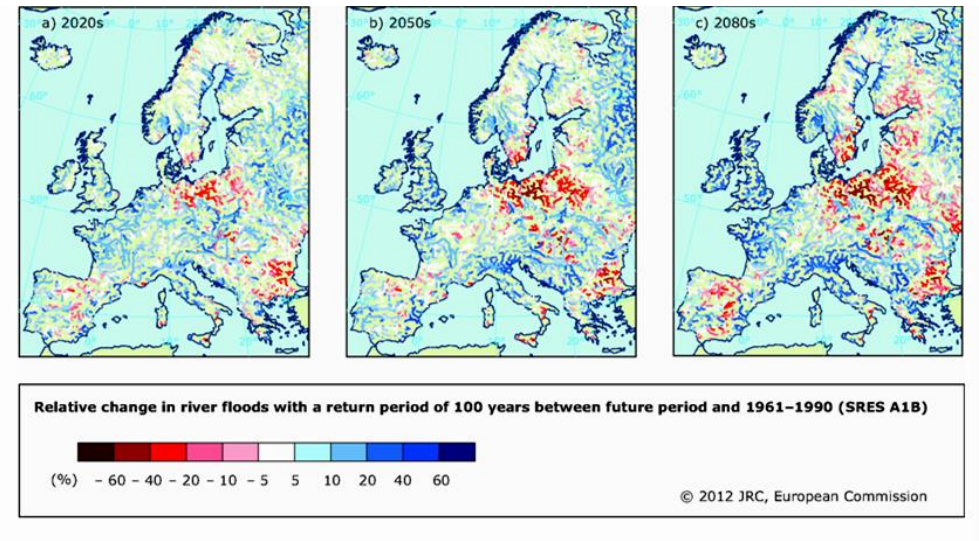

Figure 37 *Relative change in minimum river flow for a) 2020s, b) 2050s and c) 2080s compared to 1961-1990 for SRES A1B scenario (EEA, 2012)*

In Fig. 38 the flood risk by region is shown. CV & C is projected to increases by > 50% the numbers of people affected by the current 30-year flood. By the 2050s, there is at least a 50 % chance that climate change alone could lead to a 50 % increase in flooded people across sub-Saharan Africa, and a 30 - 70 % chance that such an increase would also take place in Asia. By 2100, risks will be higher. Population change alone will increase the numbers of people affected by flooding. The global total increases very substantially (by about 5 - 6 times) over the century for the business as usual (RCP8.5) scenario (King et al., 2015).

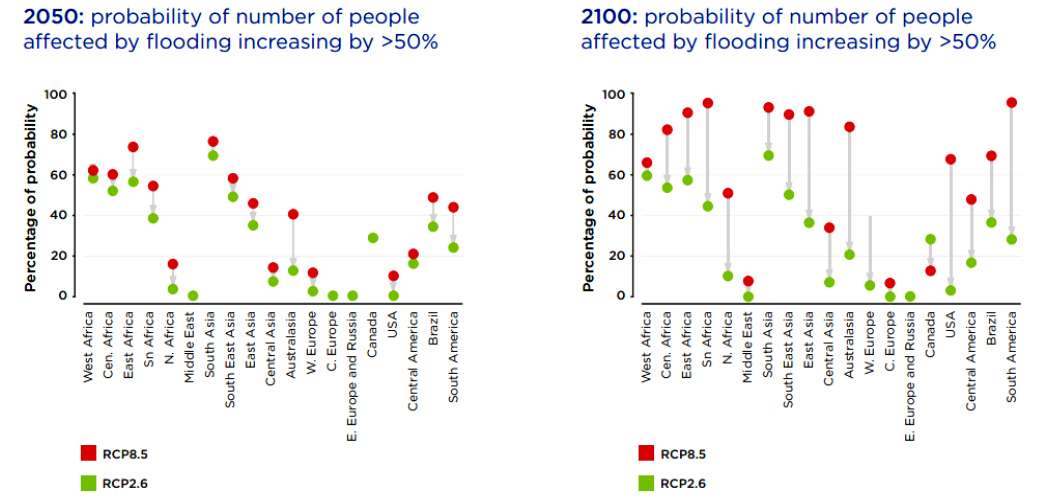

Figure 37 *Probability that climate change will increase by more than 50% the number of people affected by the current 30-year flood, relative to the situation with no climate change, under two RCPs. Medium growth population projection is assumed (King et al., 2015)*

Concerning the UNECE region, flood impacts in 2050 are projected to be generally milder than in the other regions; nevertheless, the situation for some UNECE regions is projected to deteriorate in 2100 (Fig. 38).

1.3. Summary

In this Chapter a review of the long-term and recent trends and variability of different climatic factors that can affect transportation has been presented, together with a review of the recent projections on the evolution of these factors in the 21st century under different emission scenarios. The major findings are summarized below.

Trends

There is overwhelming evidence for a warming world since the 19th century from scientific observations from the upper atmosphere to the ocean deeps. The global average surface temperature has risen by 1.1 ^{0}C since the late 19th century, with the most recent period (2012 -2017) being the warmest on record. 2016 has also been the hottest year on record (1.1 °C higher than the 1901-2000 average of 14.0 ^{0}C), whereas 2017, although an neutaral El Niño year has been the third warmest on record (after 2016 and 2015). In the UNECE region, temperatures were more than 1 °C above the 1961-1990 average over most of Europe, northern Asia and the southwestern US and reaching about 3 °C above average in regions of the Russian Arctic. The integrated ocean heat content within the upper (0 - 700 m) and intermediate ocean (to 2000 m depth) layers was higher than any previous time and sea surface temperatures (SSTs) were above average in most of the oceans. Evidence suggests that warm extremes have become warmer and cold extremes less cold in many regions.

Land precipitation data reveal an increasing trend in the 20th Century, especially in mid and high latitudes and a strong regional variability which, in many cases, appears to be influenced by the large climatic modulations such as the ENSO and NAO. Land precipitation in the most recent period was strongly influenced by the ENSO, i.e. the La Niña conditions in 2011-2012, and the strong El Niño of 2015-2016. In 2016, precipitation above the 90th percentile was observed in a large swath of land extending from Kazakhstan across the western Russian Federation into Finland, N. Sweden and Norway; at the same time, large areas of the northern and central Russian Federation were dry, with much of the region between the Urals and Lake Baikal and to the north of 55 ^{0}N showing precipitation below the 10th percentile.

There has been also an increase in heavy precipitation events (in intensity and/or frequency) in many areas of the UNECE region. One of the clearest trends appears to be the increasing frequency/intensity of heavy downpours in areas that there is already a significant flood risk (for the 1 in a 100-year events), such as the central and eastern Europe, central Asia and along the large S-N drainage basins of Siberia. Consequently, flood damages are expected to rise considerably by the end of the century, being generally higher in the north than in the south. In some regions, there is also evidence to suggest increases in the frequency/intensity of heat waves (e.g. in the Mediterranean and the southwestern USA).

Over the past few decades, there appears to be a downward trend in the extent/duration of snow cover in the Arctic. Snow cover has declined (in the month of June) by 11.7 % per decade over the period 1967-2012. However, this trend is not uniform; some regions (e.g. the Alps and Scandinavia) show consistent decreases at low elevations but increases at high elevations, whereas other regions (e.g. the Carpathians, Pyrenees, and Caucasus) show no consistent trends. There has been a decrease in the number of frost days in mid-latitude regions. Arctic sea ice continued its steep decline. In 2016, sea ice extent (SIE) was well below average and at record low levels for large parts of the year; March seasonal maximum was

14.52 million km^2, the lowest seasonal maximum in the 1979–2016 satellite record. In 2017, SIE was also well below the 1981 – 2010 average in both the Arctic and Antarctic. Mountain glaciers also continued to decline. Permafrost extent also continued to decrease; recently, there has been warming down to 20 m depth in Arctic permafrost regions.

Since 1860, sea level has increased by about 0.20 m, with the rate of increase becoming progressively greater, particularly since the 1990s. SLR trend over the satellite record (1993-2015) has been 3-3.3 mm yr^{-1}, considerably higher than the 1900-2010 average (1.7 mm year^{-1}).

Extreme hydro-meteorological events (e.g. heat and cold waves, tropical cyclones, floods, droughts and intense storms) causing significant losses/damages also appear to be on the rise; fortunately, human loss did not follow the steep upward trend of the economic losses associated with these extreme events. The 2017 hurricane season which affected the southern USA and overseas territories of UNECE Member States in the Caribbean has ben assessed as the mostly costly on record (US$ 265 billion)

Projections

Recent projections on the climatic factors that could impact transport infrastructure and operations are presented below. Generally, challenges that are already imposed by certain climatic factors on the present day transport infrastructure will increase significantly.

By the end of the 21st century, the mean atmospheric temperature is projected to increase between 1.0 and 3.7 °C above the mean temperature of the period 1986–2005, depending on the RCP scenario. Oceans will warm under all scenarios, with the highest SSTs projected for the subtropical and tropical regions. Increases in hot extremes and decreases in cold extremes are expected by the end of the 21th century, particularly in mid-latitude regions. Large regional differences are projected for temperature maxima (TX_X); these may increase in central Europe, central N. America and N. Australia. The frequency/duration of heat waves is projected to increase for many regions (and in Europe), particularly under high emission scenarios. For most land regions it is considered likely that the frequency of the current 20-year hot event will be doubled; in some areas, such an event might even occur every 1-2 years. At the same time, the occurrence of the current 20-year cold event will substantially decrease in the future.

As temperature rises, average precipitation will exhibit substantial spatial variation in its patterns. Land precipitation is projected to increase in high and mid latitudes and decrease in sub-tropical arid and semi-arid regions. Extreme precipitation events will likely be more intense over most of the mid-latitude and wet tropical regions. For central and NE Europe, projections demonstrate large increases (by 25 %) in heavy precipitation events by the end of the century. At the same time, widespread droughts across most of southwestern North America are projected for the mid to late 21st century. In comparison, decreases are projected for the duration/intensity of droughts in southern Europe and the Mediterranean, central Europe and other areas of North America.

Snowfall and rainfall are projected to increase in the Arctic regions, mostly in winter. However, although winter maximum snow depth will likely increase (particularly in Siberia), early melt will result in considerable decreases (by up to 25 %) in spring snow cover in the Northern Hemisphere (NH). Mountain glaciers and ice caps are projected to show a 10 to 30 % mass reduction by the end of the century. Models also project accelerating thawing of permafrost, due to rising temperatures and changes in snow cover. Current rates of warming of the European permafrost surface are 0.04 – 0.07 °C yr^{-1} and, although there are

challenges in assessing permafrost change, its extent in 2100 is expected (medium confidence) to decrease by 37 % and 81 % for the RCP2.6 and RCP8.5 scenarios, respectively.

It is also likely that the Arctic sea ice will continue to decrease in extent/thickness, although there will be considerable inter-annual variability. In the period 2081 - 2100, reductions in Arctic ice extent of 8 to 34 % (in February) and of 43 to 94 % (in September) are projected (compared to the average extents in 1986 - 2005) for RCP2.6 and RCP8.5. These may result in the development of major Arctic shipping routes which, however, could be associated with environmental risks and development difficulties, such as those imposed by the projected permafrost thaw on the development/maintenance of the necessary coastal and land transport infrastructure to service these routes.

CV & C risks to the UNECE coastal transport infrastructure are also expected to rise. Sea level rise for the ECE region depends on the emission scenario, with greater rises predicted in the case of additional (land) ice sheet melting. In the North Sea coast, for instance, mean sea level rises of 0.40 to 1.05 m are expected, with slightly lower rates projected for the Mediterranean coast. Larger storm surge levels are projected for the Atlantic, North Sea and Baltic coasts (and seaports) under all scenarios and extreme storm events. For southern Europe, however, projections are better, with expected changes in the storm surge and extreme sea levels mostly in the ±5 % band.

Recent research suggests a negative trend in the wave energy fluxes-WEF (for the 100-year return event) along the UNECE coast, with the exception of the NE Pacific and the Baltic coasts which are projected to show increases of up to 30 %. With regard to the extreme sea levels (ESLs) and taking into account the presence/standards of coastal flood protection works and uncertainties concerning the probability of their failure, about 5 million people in Europe could potentially be affected by the present day 100-year ESL. Averaged over Europe's coastlines, such an event is projected to occur approximately every 11 years by 2050, and every 1 to 3 years by 2100 (RCP4.5 and RCP8.5). Coastal transport infrastructure currently at risk once every 100 years may face flooding at an almost annual basis by the end of the century. Some regions are projected to experience an even higher increase in the frequency of occurrence of extreme events, most notably along the Mediterranean and the Black Sea; in these areas, such events are projected to occur even more often.

It appears that the effects of these events on the coastal transportation infrastructure (and related supply chains) should be urgently assessed in more detail. It should be also noted that as the current trend in climatic research is to assess impacts in relation to temperature thresholds (e.g. IPCC, 2018), it would be very useful to understand/communicate the CV & C implications on the infrastructure and activities for given global temperature targets (Seneviratne et al., 2016).

References

Alfieri, L., Feyen, L., Dottori, F. and Bianchi A., 2015. Ensemble flood risk assessment in Europe under high end climate scenarios. Global Environmental Change 35,199-212. (doi:10.1016/j.gloenvcha.2015.09.004)

Alfieri, L., Dottori, F., Betts, R., Salamon, P., Feyen, L., 2018. Multi-model projections of river flood risk in Europe under global warming. Climate 6, 16 doi:10.3390/cli6010016

AMAP, 2012. Arctic Climate Issues 2011: Changes in Arctic Snow, Water, Ice and Permafrost. SWIPA 2011.Overview Report

Androulidakis, Y.S., Kombiadou, K.D., Makris, C.H., Baltikas, V.N. and Krestenitis, Y.N. 2015 Storm surges in the Mediterranean Sea: Variability and trends under future climatic conditions. Dynamics of Atmospheres and Oceans 71, 56–82.

Arnell N. et al 2014. Global-scale climate impact functions: the relationship between climate forcing and impact. Climate Change (134), 475–87.

Asariotis R., Mohos-Naray V., Benamara H., 2017. Port Industry Survey on Climate Change Impacts and Adaptation. UNCTAD Research Paper No. 18, UNCTAD/SER.RP/2017/18. 37 pp plus Appendices.
https://unctad.org/en/PublicationsLibrary/ser-rp-2017d18_en.pdf

Beniston, M. and Diaz, H.F. 2004. The 2003 heat wave as an example of summers in a greenhouse climate? Observations and climate model simulations for Basel, Switzerland. Global and Planetary Change 44, 73-81.

Bertin, X., Prouteau, E. and Letetrel, C. 2013. A significant increase in wave height in the North Atlantic Ocean over the 20th century. Global and Planetary Change 106, 77–83.

Camus, P., Losada, I.J., Izaguirre, C., Espejo, A., Menéndez, M., Pérez, J., 2017. Statistical wave climate projections for coastal impact assessments. Earth's Future 5, 918–933. https://doi.org/10.1002/2017EF000609

Canadell J.G., Le Quere C., Raupach M.R., Field C.R., Buitenhuis E., Ciais P., Conway T.J., Gillett N.P., Houghton R.A. and Marland G., 2007. Contributions to accelerating atmospheric CO2 growth from economic activity, carbon intensity, and efficiency of natural sinks. Proceedings of the National Academy of Sciences 104, 18866-18870.

Carson M., Kohl A., Stammer D., Slangen A.B.A., Katsman C.A., van de Wal R.S.W., Church, J. and White, N. 2016. Coastal sea level changes, observed and projected during the 20th and 21st century. Climatic Change 134, 269-281. (doi: 10.1007/s10584-015-1520-1).

Cheng, L., Abraham, J., Hausfather, Z., Trenberth, K.E., 2019a. How fast are the oceans warming? Observational records of ocean heat content show that ocean warming is accelerating. Science 363 (6423), 128-129.

Cheng, L., Zhu, J., Abraham, J., Trenberth, K.E. Fasullo, J.T., Zhang, B., Yu, F., Wan, L., Chen, X., Song, X., 2019b. 2018 Continues Record Global Ocean Warming. Advances in Atmospheric Sciences 36 (3), 249–252. https://doi.org/10.1007/s00376-019-8276-x

Church, J. A. and White, N. J. 2006. A 20th century acceleration in global sea-level rise. Geophysical Research Letters 33, L01602. (doi:10.1029/2005GL024826)

Church J.A., Clark P.U., Cazenave A., Gregory J.M., Jevrejeva S., Levermann A., Merrifield M.A., Milne G.A., Nerem R.S., Nunn P.D.. Payne A.J., Pfeffer W.T.. Stammer D., Unnikrishnan A.S., 2013. Sea level change. In Climate Change 2013: The Physical Science Basis. Contribution of Working Group I to the Fifth Assessment Report of the Intergovernmental Panel on Climate Change. (T.F. Stocker, Qin D., Plattner G.-K., Tignor M., Allen S.K., Boschung J., Nauels A., Xia Y., Bex V., Midgley P.M. [eds]) Cambridge; UK 1137-1216.

Conte, D. and Lionello, P. 2014. Storm Surge Distribution Along the Mediterranean Coast: Characteristics and Evolution , Procedia -Social and Behavioral Sciences 120, 110-115. (ISSN 1877-0428).

Coumou, D. and Rahmstorf, S. 2012. A decade of weather extremes. Nature Climate Change 29, 491-496. (doi:10.1038/nclimate1452).

Coumou D. and Robinson A., 2013. Historic and future increase in the global land area affected by monthly heat extremes. Environmental Research Letters 8 (3) http://iopscience.iop.org/article/10.1088/1748-9326/8/3/034018/meta.

Cowtan, K. and Way, R. G. 2014. Coverage bias in the HadCRUT4 temperature series and its impact on recent temperature trends. Q.J.R. Meteorol. Soc. 140, 1935–1944. (doi: 10.1002/qj.2297)

Cronin, T.M. 2012. Rapid sea-level rise. Quaternary Science Reviews 56, 11-30.

Dai, A. 2013. Increasing drought under global warming in observations and models. Nature Climate Change 3, 52–58.

De Conto, R.M. and Pollard. D. 2016. Contribution of Antarctica to past and future sea-level rise. Nature 531, 591-596. (doi: 10.1038/nature17145)

Dieng H.B., A. Cazenave, B. Meyssignac, K. von Schuckmanc and H. Palanisamya, 2017a. Sea and land surface temperatures, ocean heat content, Earth's energy imbalance and net radiative forcing over the recent years. Int. J. Climatol. (2017), 12 pp., doi: 10.1002/joc.4996

Dieng, H. et al., 2017b: New estimate of the current rate of sea level rise from a sea level budget approach. Geophysical Research Letters, 44, doi: 10 .1002/ 2017GL073308.

Dole et al., 2011. Was there a basis for anticipating the 2010 Russian heat wave? Geophysical Research Letters 38, L06702.

Domingues, C.M., Church, J.A., White, N.J., Gleckler, P.J., Wijffels, S.E., Barker, P.M. and Dunn, J.R. 2008. Improved estimates of upper-ocean warming and multi-decadal sea-level rise. Nature 453, 1090-1094.

Dutton A., ,A. E. Carlson, A. J. Long, G. A. Milne, P. U. Clark, R. DeConto, B. P. Horton, S. Rahmstorf, and M. E. Raymo, 2015. Sea-level rise due to polar ice-sheet mass loss during past warm periods. Science 349, 6244 https://marine.rutgers.edu/pubs/private/Science-2015-Dutton-.pdf

EC, 2012. Impacts of Climate Change on Transport: A focus on road and rail transport infrastructures, (F. Nemry and H. Demirel), JRC Scientific and Policy Reports. Publications Office of the European Union, Luxembourg, ISBN 978-92-79-27037-6.

ECE, 2013. Climate Change Impacts and Adaptation for International Transport Networks, United Nations Economic Commission for Europe, New York and Geneva, 2013, 248 pp. http://www.unece.org/fileadmin/DAM/trans/main/wp5/publications/climate_change_2014.pdf

ECE, 2015. Transport for Sustainable Development: The case of Inland Transport. United Nations Economic Commission for Europe, Transport Trends and Economics Series ECE/TRANS/251. http://www.unece.org/fileadmin/DAM/trans/publications/Transport_for_Sustainable_Development_UNECE_2015.pdf

EEA, 2010. The European environment: State and outlook 2010, Adapting to climate change. European Envronmental Agency, Copenhagen. (ISBN 978-92-9213-159-3).

EEA, 2012. Climate change, impacts and vulnerability in Europe 2012. An indicator-based report. European Environmental Agency (EEA), Copenhagen, Denmark, 300 pp. (ISBN 978-92-9213-346-7)

EEA, 2014a. Projected changes in annual, summer and winter temperature. [Online image]. European Environment Agency (EEA). Available from: http://www.eea.europa.eu/data-and-maps/figures/projected-changes-in-annual-summer-1 [Accessed 01/03/2016].

EEA, 2014b. Trend in absolute sea level in European Seas based on satellite measurements (1992–2013). [Online image]. European Environment Agency (EEA). Available from: http://www.eea.europa.eu/data-and-maps/figures/sea-level-changes-in-europe-october-1992-may-1 [Accessed 01/03/2016].

EEA, 2014c. Projected change in relative sea level. [Online image]. European Environment Agency (EEA). Available from: http://www.eea.europa.eu/data-and-maps/figures/projected-change-in-sea-level [Accessed 01/03/2016].

EEA, 2015a, Global megatrends assessment: Extended background analysis complementing the SOER 2015 'Assessment of global megatrends'. European Environmental Agency, Copenhagen. (ISSN 1725-2237).

EEA, 2015b. Number of extreme heat waves in future climates under two different climate forcing scenarios. Available from: http://www.eea.europa.eu/data-and-maps/figures/number-of-extreme-heat-waves [Accessed 13/07/2015].

EEA, 2015c. Projected changes in heavy precipitation (in %) in winter and summer from 1971-2000 to 2071–2100 for the RCP8.5 scenario based on the ensemble mean of different regional climate models (RCMs) nested in different general circulation models (GCMs). Available from: http://www.eea.europa.eu/data-and-maps/figures/projected-changes-in-20-year-2 [accessed 21/03/2016].

Emanuel, K. 2005. Increasing destructiveness of tropical cyclones over the past 30 years. Nature 436, 686-688.

Engelhart, S.E., Horton, B.P., Douglas, B.C., Peltier, W.R. and Törnqvist, T.E. 2009. Spatial variability of late Holocene and 20th century sea-level rise along the US Atlantic coast. Geology, 37, 1115-1118.

EPA, 2015. Precipitation Worlwide, 1901-2013 [Online image]. Available from: https://www3.epa.gov/climatechange/science/indicators/weather-climate/precipitation.html [Accessed 03/02/2016].

Feyen L, Dankers R and Bodis K, 2010. Climate warming and future flood risk in Europe. Climatic Change.

Forzieri, G., Feyen, L., Russo, S. et al. 2016. Multi-hazard assessment in Europe under climate change. Climatic Change 137, 105 - 119. https://doi.org/10.1007/s10584-016-1661-x.

Fourier J. J., 1827. MEMOIRE sur les temperatures du globe terrestre et des espaces planetaires Memoires d l'Academie Royale des Sciences de l'Institute de France VII, pp. 570–60.

Fyfe J.C., Meehl G.A., England M.H., Mann M.E., Santer B.D., Flato G.M., Hawkins E., Gillett N.P., Xie S-P., Kosaka Y. and Swart N.C, 2016. Making sense of the early-2000s warming slowdown. Nature Climate Change 6, 224–228, doi:10.1038/nclimate2938.

Gehrels, W.R. and Woodworth, P.L. 2012. When did modern rates of sea-level rise start? Global Planetary Change 100, 263-277.

GISTEMP, 2016. NASA Goddard Institute for Space Studies - GISS Surface Temperature Analysis (GISTEMP). Available from : http://data.giss.nasa.gov/gistemp/.

Grinsted A, Moore JC and Jervejeva S, 2010. Reconstructing sea level from paleo and projected temperatures 200 to 2100 AD. Climate Dynamics 34, 461- 472.

Hallegatte, S., Green, C., Nicholls, R. J. and Corfee-Morlot, J. 2013. Future flood losses in major coastal cities,Nature Climate Change 3, 802–806. (doi:10.1038/NCLIMATE1979)

Hanna, E. et al., 2013. Ice sheet mass balance and climate change. Nature 498, 51-59.

Hansen, J., Sato, M., Hearty, P., Ruedy, R., Kelley, M., Masson-Delmotte, V., Russell, G., Tselioudis, G., Cao, J., Rignot, E., Velicogna, I., Tormey, B., Donovan, B., Kandiano, E., von Schuckmann, K., Kharecha, P., LeGrande, A.N., Bauer, M. and K.-W. Lo. 2016. Ice melt, sea level rise and superstorms: Evidence from paleoclimate data, climate modeling, and modern observations that 2°C global warming could be dangerous. Atmos. Chem. Phys. 16, 3761-3812 (doi:10.5194/acp-16-3761-2016).

Hay, C.C., Morrow, E., Kopp, R.E. and Mitrovica, J.X. 2015. Probabilistic reanalysis of twentieth-century sea-level rise. Nature 517, 481-484.

Hinkel, J., Lincke, D., Vafeidis, A. T., Perrette, M., Nicholls, R. G.,Tol, R. S., Marzeion, B., Fettweis, X., Ionescu, C., and Levermann, A, 2014. Coastal flood damages and adaptation costs under 21st century sea-level rise, Proceedings of the National Academy of Sciences USA, 111, 3292–3297,

Horton R., Herweijer C, Rosenzweig C, Liu J, Gornitz V, and Ruane AC, 2008. Sea level rise projections for current generation CGCMs based on the semi-empirical method. Geophysical Research Letters 35 DOI:10/1029/2007GL032486.

Horton, B.P., Rahmstorf, S., Engelhart, S.E. and Kemp, A.C. 2014. Expert assessment of sea-level rise by AD 2100 and AD 2300. Quaternary Science Reviews, 84, 1-6.

IPCC, 2007. Climate Change 2007. The Physical Science Basis. Contribution of Working Group I to the Fourth Assessment Report of the Intergovernmental Panel on Climate Change (Solomon S, D Qin, M Manning, Z Chen, M Marquis, KB Averyt, M Tignor and HL Miller (eds)). Cambridge University Press, Cambridge, UK and New York, NY, USA, 996 pp.

IPCC, 2013. Climate Change 2013: The Physical Science Basis. Contribution of Working Group I to the Fifth Assessment Report of the Intergovernmental Panel on Climate Change [Stocker, T.F., D. Qin, G.-K. Plattner, M. Tignor, S.K. Allen, J. Boschung, A. Nauels, Y. Xia, V. Bex and P.M. Midgley (eds.)]. Cambridge University Press, Cambridge, United Kingdom and New York, NY, USA.

IPCC, 2014. Summary for policy makers. In: Climate Change 2014: Impacts, Adaptation, and Vulnerability. Part A: Global and Sectoral Aspects. Contribution of Working Group II to the Fifth Assessment Report of the Intergovernmental Panel on Climate Change [Field, C.B., V.R. Barros, D.J. Dokken, K.J. Mach, M.D. Mastrandrea, T.E. Bilir, M. Chatterjee, K.L. Ebi, Y.O. Estrada, R.C. Genova, B. Girma, E.S. Kissel, A.N. Levy, S. MacCracken, P.R. Mastrandrea, and L.L. White (eds.)]. Cambridge University Press, Cambridge, United Kingdom and New York, NY, USA, pp. 1-32.

IPCC, 2018: Summary for Policymakers. In: Global warming of 1.5°C. An IPCC Special Report on the impacts of global warming of 1.5°C above pre-industrial levels and related global greenhouse gas emission pathways, in the context of strengthening the global response to the threat of climate change, sustainable development, and efforts to eradicate poverty [V. Masson-Delmotte, P. Zhai, H. O. Pörtner, D. Roberts, J. Skea, P. R. Shukla, A. Pirani, W. Moufouma-Okia, C. Péan, R. Pidcock, S. Connors, J. B. R. Matthews, Y. hen, X. Zhou, M. I. Gomis, E. Lonnoy, T. Maycock, M. Tignor, T. Waterfield (eds.)]. World Meteorological Organization, Geneva, Switzerland 32 pp. https://www.ipcc.ch/site/assets/uploads/sites/2/2018/07/SR15_SPM_High_Res.pdf

IPCC SREX, 2012. Managing the Risks of Extreme Events and Disasters to Advance Climate Change Adaptation [Field, C.B., V. Barros, T.F. Stocker, D. Qin, D.J. Dokken, K.L. Ebi, M.D. Mastrandrea, K.J. Mach, G.-K. Plattner, S.K. Allen, M. Tignor, and P.M. Midgley (eds.)]. A Special Report of Working Groups I and II of the Intergovernmental Panel on Climate Change (IPCC). Cambridge University Press, Cambridge, UK, and New York, NY, USA. 582 pp.

Jevrejeva S, Moore JC and Grinsted A, 2010. How will sea level respond to changes in natural and anthropogenic forcings by 2100? Geophysical Research Letters 37. DOI: 10.1029/2010GL042947.

Jevrejeva, S., Moore, J.C. and Grinsted, A. 2012. Sea level projections to AD2500 with a new generation of climate change scenarios. Global and Planetary Change 80-81, 14-20. (doi:10.1016/j.gloplacha.2011.09.006).

Karl, T.R., Melillo, J. T. and Peterson, T. C. 2009. Global Climate Change Impacts in the United States.. Cambridge University Press, 189 pp.

Karl, T.R., Arguez, A., Huang, B., Lawrimore, J.H., McMahon, J.R., Menne, M.J., Peterson, T.C., Vose, R.S. and Zhang, H. 2015. Possible artifacts of data biases in the recent global surface warming hiatus, Science, 348, pp. 1469-1472.

Katsman, C.A., Sterl, A., Beersma, J.J., Brink, H.W., Church, J.A., Hazeleger, W., Kopp, R.E., Kroon, D., Kwadijk. J., Lammersen, R., Lowe, J., Oppenheimer, M., Plag, H.P., Ridley. J., Storch, H. et al., 2011. Exploring high end scenarios for local sea level rise to develop flood protection strategies for a low-lying delta. The Netherlands as an example. Climatic Change 109 (3-4), 617–645. (doi:10.1007/s10584-011-00375)

King, D., Schrag, D., Dadi, Z., Ye, Q. and Ghosh, A. 2015. Climate Change: A Risk Assessment. Centre for Science and Policy, University of Cambridge. (http://www.csap.cam.ac.uk/media/uploads/files/1/climate-change--a-risk-assessment-v9-spreads.pdf)

Kopp R, Simons F, Mitrovica J, Maloof A and Oppenheimer M. 2009. Probabilistic assessment of sea levelduring the last interglacial stage. Nature 462, 863–867. (doi:10.1038/nature08686).

Lionello, P., Galati, M.B. and Elvini, E. 2012. Extreme storm surge and wind wave climate scenario simulations at the Venetian littoral. Phys Chem Earth Parts A/B/C 40–41, 86–92.

Losada, I.J., Reguero, B.J., Mendez, F.G., Castanedo, S., Abascal, A.J. and Minguez, R. 2013. Long-term changes in sea level components in Latin America and the Caribbean. Global and Planetary Change 104, 34–50.

Lyman, J. M. et al. 2010. Robust warming of the global upper ocean, Nature, 465, pp. 334–337.

Marcos, M., Jorda, G., Gomis, D. and Perez, B. 2011. Changes in storm surges in southern Europe from a regional model under climate change scenarios. Global and Planetary Change 77(3–4), 116–128. (doi:10.1016/j.gloplacha.2011.04.002)

Mel, R., Sterl, A. and Lionello, P. 2013. High resolution climate projection of storm surge at the Venetian coast. Nat Hazards Earth System Science 13, 1135–1142.

Melillo, J.M., Richmond, T.T.C., Yohe, G.W. 2014. Climate Change Impacts in the United States: The Third National Climate Assessment. U.S. Global Change Research Program, NCA, pp. 841.

Menendez, M. and Woodworth, P.L. 2010. Changes in extreme high water levels based on a quasi-global tidegauge data set. Journal of Geophysical Research, 115, C10011. (doi:10.1029/2009JC005997).

Menounos, B., Hugonnet, R., Shean, D.et al., 2018. Heterogeneous Changes in western North American glaciers linked to decadal variability in zonal wind strength. Geophysical Research Letters 45, https://doi.org/10.1029/2018GL08094.

Mentaschi, L., M. I. Vousdoukas, E. Voukouvalas, A. Dosio, and L. Feyen, 2017. Global changes of extreme coastal wave energy fluxes triggered by intensified teleconnection patterns. Geophys. Res. Let. 44, 2416–2426, doi:10.1002/2016GL072488.

MetOffice, 2014. Climate risk An update on the science. Met Office, Handley Center, Devon, UK, 9 pp.

Meyer-Christoffer, A.; Becker, A.; Finger, P.; Rudolf, B.; Schneider, U.; Ziese, M. GPCC Climatology Version 2015 at 0.25◦: Monthly Land-Surface Precipitation Climatology for Every Month and the Total Year from Rain-Gauges Built on GTS-Based and Historic Data; GPCC: Offenbach, Germany, 2015.

Milly, P.C.D., Betancourt, J., Falkenmark, M., Hirsch, R.M., Kundzewicz, Z.W., Lettenmaier D.P. and Stouffer, R.J. 2008. Stationarity is dead: Whither water management? Science 319, 573-574.

Monioudi I., N., Asariotis R., Becker A. et al., 2018. Climate change impacts on critical international transportation assets of Caribbean Small Island Developing States (SIDS): The case of Jamaica and Saint Lucia. Regional Environmental Change, 18 (8), 2211–2225.

Mora, C., Dousset, B., Caldwell, I.R. et al., 2017. Global risk of deadly heat. Nature Climate Change 7, 501-507. DOI: 10.1038/NCLIMATE3322

Mori N, Shimura T, Yasuda T and Mase H, 2013. Multi-model climate projections of ocean surface variables under different climate scenarios—Future change of waves, sea level and wind. Ocean Engineering, http://dx.doi.org/10.1016/j.oceaneng.2013.02.016i

Moss R, et al., 2010. The next generation of scenarios for climate change research and assessment. Nature 463, 747–756.

Munich Re, 2015. NatCatSERVICE: Loss events worldwide 1980-2014.

NASA, 2016. NOAA Analyses Reveal Record-Shattering Global Warm Temperatures in 2015 [WWW] Goddard Institute for Space Studies. Available from: http://www.giss.nasa.gov/research/news/20160120/ [Accessed 13/02/2016]

NOAA, 2015. 2014 State of the Climate: Carbon Dioxide [WWW] Available from: https://www.climate.gov/news-features/understanding-climate/2014-state-climate-carbon-dioxide

NOAA, 2016a. Global Analysis - Annual 2015: 2015 year-to-date temperatures versus previous years [WWW] National Centers for Environmental Information. Available from: https://www.ncdc.noaa.gov/sotc/global/2015/13/supplemental/page-3 [Accessed 122/02/2016]

NOAA, 2016b. Global Analysis - November 2015 [WWW] National Centers for Environmental Information. Available from: https://www.ncdc.noaa.gov/sotc/global/201511 [Accessed 122/02/2016]

NOAA, 2016c. Global Analysis - February 2016 [WWW] National Centers for Environmental Information. Available from: https://www.ncdc.noaa.gov/sotc/global/201602 [Accessed 122/02/2016].

NOAA, 2016d. Global Analysis - February 2016 [WWW] National Centers for Environmental Information. Available from: https://www.ncdc.noaa.gov/sotc/global/201602 [Accessed 12/02/2016]

NOAA, 2017a. National Center for Environmental Information (NCEI), State of the Climate: Global Snow and Ice for 2016. (Published online 01/2017, retrieved on May 9, 2017 from https://www.ncdc.noaa.gov/sotc/global-snow/201613

NOAA, 2017b. National Centers for Environmental Information (NCEI). 2016 Officially Warmest Year on Record. (Published online January 2017, accessed on May 24, 2017 https://www.nnvl.noaa.gov/MediaDetail2.php?MediaID=1989&MediaTypeID=3&ResourceID=105007/

NOAA, 2017c. National Centers for Environmental Information (NCEI) U.S. Billion-Dollar Weather and Climate Disasters. https://www.ncdc.noaa.gov/billions/

NSIDC, 2012. Rapid sea ice retreat in June [WWW] National Snow & Ice Data Center. Available from: http://nsidc.org/arcticseaicenews/2012/07/rapid-sea-ice-retreat-in-june/ [accessed 15/02/2016]

NSIDC, 2017. National Snow and Ice Data Center. Snow, Ice and Climate Change (retrieved on May 24, 2017 from http://nsidc.org/cryosphere/climate-change.html

Perherin, C., A. Roche, F. Pons, I. Roux, G. Desire, and C. Boura (2010). Vulnérabilité du territoire national aux risques littoraux. XIèmes Journées Nationales Génie Côtier – Génie Civil Les Sables d'Olonne, 22-25 June 2010. (doi: 10.5150/jngcgc.2010.072-P).

Pérez, J., Menendez, M., Mendez, F. and Losada, I. 2014. Evaluating the performance of CMIP3 and CMIP5 global climate models over the north-east Atlantic region. Climate Dynamics 43, 2663–2680.

Pfeffer W, Harper J and O' Neel S, 2008. Kinematic constraints on glacier contributions to 21st century sea levelrise. Science 321, 1340–1343. (doi:10.1126/science.1159099).

Pritchard, H.D., Ligtenberg, S.R.M., Fricker, H.A., Vaughan, D.G., van den Broeke, M.R. and Padman, L. 2012. Antarctic ice-sheet loss driven by basal melting of ice shelves. Nature 484, 502–505.

Rahmstorf S, Cazenave A, Church JA, Hansen JE, Keeling RF, Parker DE, and RCJ Somerville, 2007. Recent climate observations compared to projections. Science 316, 709-709.

Rahmstorf S., 2012. Climate Change: State of Science . In: Maritime Transport and the Climate Change Challenge, R. Asariotis and H. Benamara, eds., Earthscan, pp. 3-11.

Rahmstorf S., Foster G., Cahill N, 2017. Global temperature evolution: recent trends and some pitfalls. Environmental Research Letters 12, 054001.

Ranasinghe, R., 2016. Assessing climate change impacts on open sandy coasts: A review. Earth Science Reviews 160, 320-332.

Raper, S.C.B. and Braithwaite, R. J. 2009. Glacier volume response time and its links to climate and topography based on a conceptual model of glacier hypsometry. The Cryosphere 3, 183-194, (ISSN 1994-0416)

Richardson, K., Steffen, W., Schellnhuber, H.J., Alcamo, J., Barker, T., Kammen, D.M., Leemans, R., Liverman, D., Munasinghe, M., Osman-Elasha, B., Stern, N. and O Ole W.ver., 2009. Synthesis Report. Climate change: Global Risks, Challenges and Decisions. University of Copenhagen, 39 pp.

Rignot, E., Velicogna, I., van den Broeke, M.R., Monagha, A. and Lenaerts, J. 2011. Acceleration of the contribution of the Greenland and Antarctic ice sheets to sea level rise. Geophysical Research Letters, (38), 5 pp. (doi:10.1029/2011GL046583).

Rignot E., Mouginot, J., Scheuchl, B. et al., 2019. Four decades of Antarctic Ice Sheet mass balance from 1979–2017. PNAS https://doi.org/10.1073/pnas.1812883116

Rohling E, Grant K, Hemleben C, Siddall M, Hoogakker B, Bolshaw M and Kucera M, 2008. High rates of sea levelrise during the last interglacial period. Nature Geosciences 1, 38–42. (doi:10.1038/ngeo.2007.28).

Ruggiero, P., Komar, P.D. and Allan, J.C. 2010. Increasing wave heights and extreme value projections: The wave climate of the U.S. Pacific Northwest. Coastal Engineering 57, 539–552.

Ruggiero, P. 2013. Is the intensifying wave climate of the U.S. Pacific Northwest increasing flooding and erosion risk faster than sea-level rise? Journal of Waterway, Port, Coastal, and Ocean Engineering 139 (2), 88–97.

Seneviratne, S. I., et al., 2016. Allowable CO2 emissions based on regional and impact-related climate targets. Nature 529, 477–483. doi:10.1038/nature16542.

Shakun, J.D., Clark, P.U., He, F., Marcott, S.A., Mix, A.C., Liu, Z., Otto-Bliesner, B., Schmittner, A. and Bard, E. 2012. Global warming preceded by increasing carbon dioxide concentrations during the last deglaciation, Nature 484, 49–55.

Simmons A.J., P. Berrisford, D.P. Dee, H. Hersbach, S. Hirahara and J.N. Thepaut, 2017. A reassessment of temperature variations and trends from global reanalyses and monthly surface climatological datasets. Q.J.R. Meteorol. Soc. 143, 101–119, doi:10.1002/qj.2949.

Schneider U., P.Finger, A. Meyer-Christoffer, El. Rustemeier, M. Ziese and A. Becker, 2017. Evaluating the Hydrological Cycle over Land Using the Newly-Corrected Precipitation Climatology from the Global Precipitation Climatology Centre (GPCC). Atmosphere ,8 (52), doi: 10.3390/atmos8030052.

Steffen, W. 2009. Climate Change 2009: Faster Change and More Serious Risks. Report to the Department of Climate Change, Australian Government.

Stockdon, H.F., Doran, K.J., Thompson, D.M., Sopkin, K.L., Plant, N.G. and Sallenger, A.H. 2012. National assessment of hurricane-induced coastal erosion hazards: Gulf of Mexico: U.S. Geological Survey Open-File Report 2012-1084, 51 pp.

Trenberth K.E., Cheng, L., Jacobs, P., Zhang, Y., Fasullo, J.T., 2018. Hurricane Harvey links to ocean heat content and climate change adaptation. Earth's Future 6, 730–744. https://doi.org/10.1029/2018EF000825

U.S. Climate Resilience Toolkit, 2015. Arctic Development and Transport. [WWW] Available from: https://toolkit.climate.gov/content/about-climate-resilience-toolkit (accessed 15/01/2016).

UNFCCC, 2015. The Paris Agreement by Parties to the United Nations Framework Convention on Climate Change. http://unfccc.int/meetings/paris_nov_2015/items/9445.php.

Van der Wiel K., Kapnick S.B. and Vecchi G.A., 2017. Shifting patterns of mild weather in response to projected radiative forcing. Climatic Change 140, 649-658. doi: 10.1007/s10584-016-1885-9.

Velegrakis, A.F., Trygonis, V., Chatzipavlis, A.E. et al., 2016. Shoreline variability of an urban beach fronted by a beachrock reef from video imagery. Natural Hazards, 83, Supplement 1, 201–222.

Velicogna, I., Sutterley, T. C. and van den Broeke, M. R. 2014. Regional acceleration in ice mass loss from Greenland and Antarctica using GRACE time-variable gravity data. Geophys. Res. Lett., 41(22), 8130-8137.

Vermeer M. and Rahmstorf S., 2009 Global sea level linked to global temperature. Proceedings of the National Aceademy of Sciences USA 106, 21527–21532. (doi:10.1073/pnas.0907765106).

Vogel M.M., R. Orth , F. Cheruy , S. Hagemann , R. Lorenz, B.J.J.M. van den Hurk, and S.I. Seneviratne, 2017. Regional amplification of projected changes in extreme temperatures strongly controlled by soil moisturetemperature feedbacks. Geophys. Res. Letters, 44, 1511–1519. doi:10.1002/ 2016GL071235.

Vousdoukas M.I., Voukouvalas E., Annunziato A., Giardino A. and Feyen, L., 2016a. Projections of extreme storm surge levels along Europe. Climate Dynamics doi: 10.1007/s00382-016-3019-5.

Vousdoukas M.I., E. Voukouvalas, L. Mentaschi, F. Dottori, A. Giardino, D. Bouziotas, A. Bianchi, P. Salamon and L. Feyen, 2016b. Developments in large-scale coastal flood hazard mapping. Nat. Hazards Earth Syst. Sci. 16, 1841–1853, doi:10.5194/nhess-16-1841-2016.

Vousdoukas M.I., L. Mentaschi, E. Voukouvalas, M. Verlaan, and L. Feyen, 2017. Extreme sea levels on the rise along Europe's coasts. Earth's Future 5, 304–323. doi:10.1002/2016EF000505.

Vousdoukas, M.I., Mentaschi, L., Voukouvalas, E., Verlaan, M., Jevrejeva, S., Jackson, L.P., Feyen, L., 2018. Global probabilistic projections of extreme sea levels show intensification of coastal flood hazard. Nat. Commun. 9, 2360. https://doi.org/10.1038/s41467-018-04692-w.

Wada, Y., van Beek, L.PH., Weiland, FCS., Chao, B.F., Wu, Y-H. and Bierkens, MFP. 2012. Past and future contribution of global groundwater depletion to sea-level rise. Geophys Res Letters 39, L09402. (doi: 10.1029/2012GL051230)

Valdes-Abellan J., Pardo M.A. and Tenza-Abril, 2017. Observed precipitation trend changes in the western Mediterranean region. Int. J. Climatol. doi: 10.1002/joc.4984.

Vellinga P et al. 2008. Exploring high-end climate change scenarios for flood protection of the Netherlands.International Scientific Assessment for the Delta Committee. SR WR-2009-05. KNMI, Alterra, The Netherlands. http://www.knmi.nl/bibliotheek/knmipubWR/WR2009-05.pdf.

WMO, 2014. Statement on the status of the global climate in 2014, World Meteorological Organization, WMO-No. 1152, Chairperson, Publications Board, Geneva, 22 pp. (ISBN: 978-92-63-11152-4.)

WMO, 2016. WMO Statement on the Status of the Global Climate in 2015, World Meteorological Organization, WMO-No. 1167, Chairperson, Publications Board, Geneva, Switzerland, 26 pp. (ISBN: 978-92-63-11167-8.). See also http://www.indiaenvironmentportal.org.in/content/421694/provisional-statement-on-the-status-of-global-climate-in-2011-2015/.

WMO, 2017. WMO Statement on the State of the Global Climate in 2016. World Meteorological Organization Report 1189, http://library.wmo.int/opac/doc_num.php?explnum_id=3414).

WMO, 2018. WMO Statement on the State of the Global Climate in 2017. World Meteorological Organization Report 1212. https://library.wmo.int/doc_num.php?explnum_id=4453.

Yan, X.-H., T. Boyer, K. Trenberth, T. R. Karl, S.-P. Xie, V. Nieves, K.-K. Tung, and D. Roemmich, 2016. The global warming hiatus: Slowdown or redistribution? Earth's Future, 4, 472–482, doi:10.1002/2016EF000417.